

A Universal Low-Complexity Symbol-to-Bit Soft Demapper

Qi Wang, Qiuliang Xie, Zhaocheng Wang, *Senior Member, IEEE*, Sheng Chen, *Fellow, IEEE*, and Lajos Hanzo, *Fellow, IEEE*

Abstract—High-order constellations are commonly used for achieving high bandwidth efficiency in most communication systems. However, the complexity of the multiplication operations associated with the standard max-sum approximation of the maximum *a posteriori* probability in the log-domain (Max-Log-MAP) symbol-to-bit demapper is very high. In this contribution, we conceive a low-complexity universal soft demapper, which reduces the demapper's complexity considerably for the binary-reflected Gray-labeled pulse amplitude modulation (PAM), phase shift keying (PSK), quadrature amplitude modulation (QAM), and amplitude phase-shift keying (APSK) relying on product constellation labeling (product-APSK). Our theoretical analysis demonstrates that the proposed demapper has exactly the same performance as the Max-Log-MAP demapper for the Gray-labeled PAM, PSK, and QAM. Our theoretical analysis and simulation results also demonstrate that for the Gray-labeled product-APSK, the performance degradation of the proposed simplified soft demapper is negligible for both 64-ary and 256-ary constellations compared with the Max-Log-MAP demapper.

Index Terms—Amplitude phase-shift keying (APSK), Max-Log-MAP, phase-shift keying (PSK), pulse amplitude modulation (PAM), quadrature amplitude modulation (QAM), soft demapper.

I. INTRODUCTION

HIGH-ORDER constellations are preferred in many transmission systems, as they are capable of achieving high bandwidth efficiency. For example, 256-ary quadrature amplitude modulation (256QAM) and 4096QAM are employed by the second-generation digital terrestrial television broadcasting standard (DVB-T2) [1] and the second-generation digital cable television broadcasting standard (DVB-C2) [2], respectively.

Manuscript received March 28, 2013; revised June 14, 2013; accepted June 30, 2013. This work was supported in part by the National Natural Science Foundation of China under Grant 61271266, by the National Key Basic Research Program of China under Grant 2013CB329203, and by the National High Technology Research and Development Program of China under Grant 2012AA011704. The review of this paper was coordinated by Prof. W. A. Hamouda.

Q. Wang and Z. Wang are with the Tsinghua National Laboratory for Information Science and Technology, Department of Electronic Engineering, Tsinghua University, Beijing 100084, China (e-mail: qiwang11@mails.tsinghua.edu.cn; zewang@mail.tsinghua.edu.cn).

Q. Xie is with the Department of Radiation Oncology, University of California, Los Angeles, CA 90024 USA (e-mail: xieqiuliang@gmail.com).

S. Chen is with Electronics and Computer Science, University of Southampton, Southampton SO17 1BJ, U.K., and also with King Abdulaziz University, Jeddah 21589, Saudi Arabia (e-mail: sqc@ecs.soton.ac.uk).

L. Hanzo is with Electronics and Computer Science, University of Southampton, Southampton SO17 1BJ, U.K. (e-mail: lh@ecs.soton.ac.uk).

Color versions of one or more of the figures in this paper are available online at <http://ieeexplore.ieee.org>.

Digital Object Identifier 10.1109/TVT.2013.2272640

Furthermore, 128QAM is recommended by the long-term evolution advanced (LTE-Advanced) standards [3], which supports reception even for high-velocity vehicular communications. However, for these high-order modulation schemes, a high-complexity symbol-to-bit demapper is required when using the conventional maximum *a posteriori* probability based in the log-domain (Log-MAP) demapping algorithm [4]. Albeit the max-sum-approximation-based version of the Log-MAP (Max-Log-MAP) demapper [5] eliminates the high-complexity exponential and logarithmic operations in the Log-MAP algorithm, the number of multiplications remains high, and the complexity of the Max-Log-MAP algorithm is on the order of $O(2^m)$, where 2^m denotes the constellation size with m representing the number of bits per symbol.

Numerous simplified demapper algorithms have been proposed for specific constellations. In [6], a bit-metric-generation approach is proposed for phase-shift keying (PSK) using Gray labeling, which recursively generates bit metrics based on a simplified function. This recursive demapper achieves the same performance as the Max-Log-MAP demapper, while reducing the number of multiplications by 59% for 32PSK. By decomposing the 2^m -ary QAM constellation into two independent ($2^{m/2}$ -ary pulse amplitude modulation (PAM) constellations, the complexity of the associated Max-Log-MAP demapper is reduced from $O(2^m)$ to $O(2^{m/2})$ [7], [8]. The complexity of the QAM demapper can be further reduced to the order of $O(m)$ by invoking a piecewise linear approximation, but this inevitably imposes performance degradation [9]. A similar soft demapper is proposed for amplitude PSK (APSK) in [10], where the constellation is partitioned with the aid of simplified hard-decision threshold (HDT)-based boundaries, and soft information is calculated as the distances between the received signal and the HDT lines. This approximate demapper reduces the number of multiplications to 4 and 11 for 16APSK and 32APSK, respectively. A simplified demapper is also proposed for multilevel coding followed by multistage decoding, which focuses on the APSK signal [11], and the complexity of this APSK demapper is reduced to a constant (neglecting comparison operations) at the cost of exponentially increasing the memory required and necessitating an additional division [11]. In [12], the complexity of the demapper is reduced by reusing the multipliers, and only 16 multipliers are used for all the four modulation modes (QPSK, 8PSK, 16APSK, and 32APSK) in the second-generation digital video broadcasting over satellite (DVB-S2) system. For the constellation rotation and cyclic Q delay modulation of DVB-T2, several simplified demappers are proposed for reducing

complexity by decreasing the number of the constellation points required for calculating the minimum squared distances [13]–[15]. For APSK using product constellation labeling (product-APSK), it is shown [16] that a $(2^{m_1} \times 2^{m_2} = 2^m)$ -ary APSK constellation can be regarded as the product of 2^{m_1} -ary PSK and pseudo 2^{m_2} -ary PAM, and a simplified demapper is proposed in [17], which reduces the complexity of the demapper from $O(2^m)$ to $O(2^{m_1}) + O(2^{m_2})$.

All the previously mentioned Gray labeling functions designed for the various constellations are the classic binary-reflected Gray labeling schemes proposed by Gray in 1953 as a means of reducing the number of bit errors, where two adjacent constellation points differ in only one bit [18]. In [19], Agrell *et al.* showed that the binary-reflected Gray labeling is the optimal labeling for PAM, PSK, and QAM, which achieves the lowest possible bit error probability among all possible labeling functions for the additive white Gaussian noise (AWGN) channel.

Against this background, in this contribution, a universal low-complexity soft demapper is proposed for various binary-reflected Gray-labeled constellations. By exploiting the symmetry of Gray-labeled constellations, we show that the complexity of a 2^m -ary demapper can be reduced from $O(2^m)$ to $O(m)$. Moreover, our proposed low-complexity soft demapper attains the same performance as the Max-Log-MAP demapper for PAM, PSK, and QAM, whereas the performance degradation of our low-complexity soft demapper is negligible for product-APSK, in comparison with the Max-Log-MAP solution.

The rest of this paper is organized as follows. In Section II, the standard Max-Log-MAP demapper is highlighted. In Section III, our simplified soft demapper is proposed, and its performance and complexity are analyzed in detail. In Section IV, the performance of both the proposed low-complexity demapper and the conventional Max-Log-MAP demapper is quantified for Gray-labeled QAM and product-APSK for transmission over both AWGN and Rayleigh fading channels. Our conclusions are drawn in Section V.

The following notations are employed throughout this contribution. Uppercase calligraphic letters denote sets, e.g., \mathcal{X} . Boldface lowercase letters represent vectors, e.g., \mathbf{b} , whose i th element is written as b_i . Uppercase letters denote random variables (RVs), e.g., X , whereas the corresponding lowercase letters represent their realizations, e.g., x . $P(x)$ is used for the probability mass function (pmf) of a discrete RV X , and $p(x)$ denotes the probability density function (pdf) of a continuous RV X . $P(y|x)$ represents the conditional pmf of $Y = y$ given $X = x$, whereas $p(y|x)$ represents the conditional pdf of $Y = y$ given $X = x$. The magnitude operator is denoted by $|\cdot|$.

II. SYSTEM MODEL WITH MAX-LOG-MAXIMUM

A POSTERIORI DEMAPPER

At the transmitter of a coded system, the coded bits are grouped into bit vectors, each with the length of m and denoted by $\mathbf{b} = (b_0 \ b_1 \ \dots \ b_{m-1})$. Bit vector \mathbf{b} is then mapped onto constellation point $x \in \mathcal{X}$ for transmission, where $\mathcal{X} = \{x_k, 0 \leq k < 2^m\}$ denotes the signal set of size 2^m .

At the receiver, the soft information for each coded bit is calculated based on received signal y , which is then passed to the decoder. For the Log-MAP demapper, the soft information on the i th bit is expressed in the form of the log-likelihood ratio (LLR) L_i according to [17]

$$\begin{aligned} L_i &= \log \frac{P(b_i = 0|y)}{P(b_i = 1|y)} = \log \frac{\sum_{x \in \mathcal{X}_i^{(0)}} P(x|y)}{\sum_{x \in \mathcal{X}_i^{(1)}} P(x|y)} \\ &= \log \frac{\sum_{x \in \mathcal{X}_i^{(0)}} p(y|x)}{\sum_{x \in \mathcal{X}_i^{(1)}} p(y|x)} \end{aligned} \quad (1)$$

for $0 \leq i < m$, where $\mathcal{X}_i^{(b)}$ denotes the signal subset of \mathcal{X} with the i th bit being $b \in \{0, 1\}$. The last equality in (1) follows from Bayes' rule and the assumption that signals $x_k, 0 \leq k < 2^m$ are equiprobable.

A flat-fading channel is modeled as $y = hx + n$, where h denotes the complex-valued channel state information (CSI), and n stands for the complex-valued AWGN with zero mean and variance $N_0/2$ per dimension. When the perfect CSI h is available at the receiver, the conditional pdf $p(y|x)$ in (1) can be written as $p(y|x) = (1/\pi N_0) \exp(-|y - hx|^2/N_0)$. Observe that given the availability of perfect CSI, the received signal can be phase equalized, after which only the amplitude of CSI h is required. Thus, we simply assume that h is nonnegative real valued. By using the well-known max-sum approximation of $\sum_j z_j \approx \max_j z_j$ for nonnegative z_j , where the summation is dominated by the largest term, the conventional Max-Log-MAP demapper is readily formulated as

$$\begin{aligned} L_i &\approx \log \frac{\max_{x \in \mathcal{X}_i^{(0)}} p(y|x)}{\max_{x \in \mathcal{X}_i^{(1)}} p(y|x)} \\ &= -\frac{1}{N_0} \left(\min_{x \in \mathcal{X}_i^{(0)}} |y - hx|^2 - \min_{x \in \mathcal{X}_i^{(1)}} |y - hx|^2 \right). \end{aligned} \quad (2)$$

The Max-Log-MAP of (2) is a fairly accurate approximation of the Log-MAP of (1) in the high signal-to-noise ratio (SNR) region, and it avoids the complex exponential and logarithmic operations. For each received signal, the Max-Log-MAP demapper calculates all the 2^m squared Euclidean distances, i.e., $|y - hx|^2$ for every $x \in \mathcal{X}$, to find the two minimum terms described in (2). Therefore, its complexity quantified in terms of multiplications is on the order of $O(2^m)$.

III. PROPOSED SIMPLIFIED SOFT DEMAPPER

After carefully examining (2), it is interesting to note that item $\min_{x \in \mathcal{X}} |y - hx|^2$, i.e., the squared Euclidean distance from received signal y to the nearest constellation point x^* , always appears in (2), and it is equal to either $\min_{x \in \mathcal{X}_i^{(0)}} |y - hx|^2$ or $\min_{x \in \mathcal{X}_i^{(1)}} |y - hx|^2$, depending on the i th bit of x^* being 0 or 1. In other words, $|y - hx^*|^2$ is always one of the two terms in (2). By denoting the bit vector that maps to signal x^* as $\mathbf{b}^* = (b_0^* \ b_1^* \ \dots \ b_{m-1}^*)$, the other item in (2) represents the squared Euclidean distance from y to the nearest constellation

179 point in subset $\mathcal{X}_i^{(\bar{b}_i^*)}$, which is denoted by $x_{i,\bar{b}_i^*}^*$, where we have

180 $\bar{b} = 1 - b$.

181 For Gray-labeled constellations, we will show that x^* and
182 $x_{i,\bar{b}_i^*}^*$, $0 \leq i < m$, can be determined by using simple compar-
183 ison and addition operations. Afterward, we only have to cal-
184 culate the $m + 1$ squared Euclidean distances, i.e., $|y - hx^*|^2$
185 and $|y - hx_{i,\bar{b}_i^*}^*|^2$ for $0 \leq i < m$. Therefore, the complexity of
186 our proposed demapper is on the order of $O(m)$.

187 Accordingly, we divide the demapping procedure into three
188 steps: 1) finding x^* and \mathbf{b}^* ; 2) determining $x_{i,\bar{b}_i^*}^*$; and
189 3) calculating L_i according to (2). For binary-reflected Gray-
190 labeled constellations, we have the following lemma from [20],
191 describing how to obtain \mathbf{b}^* .

192 **Lemma 1:** For binary-reflected Gray labeling $\mathbf{b} \rightarrow x_k$, by
193 denoting $\mathbf{c}^k = (c_0^k \ c_1^k \ \dots \ c_{m-1}^k)$ as the binary representation
194 of index k with the least significant bit (LSB) as the rightmost
195 bit, \mathbf{b} can be calculated as

$$\mathbf{b} = (c_0^k \ c_1^k \ \dots \ c_{m-1}^k) \oplus (0 \ c_0^k \ \dots \ c_{m-2}^k) \quad (3)$$

196 where \oplus represents the bitwise XOR operation.

197 The expressions generated for determining x^* and $x_{i,\bar{b}_i^*}^*$ are
198 slightly different for various constellations. In the following, the
199 simplified soft demappers designed for the Gray-labeled PAM,
200 QAM, PSK, and product-APSK are presented in detail.

201 A. PAM Demapper

202 Without loss of generality, we assume that all the signals as-
203 sociated with PAM are real valued. For the 2^m -ary Gray-labeled
204 PAM, we denote the constellation points as $x_0, x_1, \dots, x_{2^m-1}$
205 with the k th constellation point x_k given by $x_k = \delta(-(2^m -$
206 $1) + 2k)/2$, where δ denotes the distance between each pair
207 of adjacent constellation points. The detailed PAM demapping
208 procedure is given as follows.

- 209 1) *Find x^* and \mathbf{b}^* .* For 2^m -PAM, signal space can be di-
210 vided into 2^m intervals separated by amplitude thresholds
211 $-(2^{m-1} - 1)\delta, -(2^{m-1} - 2)\delta, \dots, (2^{m-1} - 1)\delta$. Mul-
212 tiplying h with the thresholds can be implemented by
213 SHIFT-ADD operations, since the thresholds are constants.
214 Additionally, we can use the binary-search algorithm to
215 find the specific interval in which y is located. Therefore,
216 only m comparison operations are required for obtaining
217 $x^* = x_{k^*}$. The corresponding bit vector \mathbf{b}^* can then be
218 calculated according to Lemma 1. An example for the
219 Gray-labeled 8PAM (Gray-8PAM) constellation is shown
220 in Fig. 1, where we have $k^* = 2$ and $\mathbf{b}^* = (0 \ 1 \ 1)$.
- 221 2) *Determine $x_{i,\bar{b}_i^*}^*$.* Considering the symmetric structure
222 of Gray-labeled PAM constellations, we have the fol-
223 lowing lemma for computing $x_{i,\bar{b}_i^*}^*$, which only requires
224 the binary representation of k^* and addition operations,
225 instead of the need to calculate all the squared Euclidean
226 distances from y to the constellation points in subset
227 $\mathcal{X}_i^{(\bar{b}_i^*)}$ and compare all the resultant 2^{m-1} metrics.

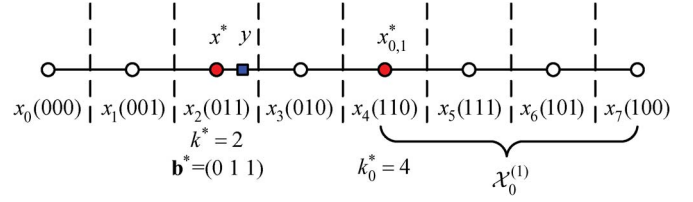


Fig. 1. Gray-8PAM constellation and illustration of demapping for the 0th bit over the AWGN channel.

Lemma 2: For the binary-reflected Gray PAM $\mathbf{b}^* \rightarrow x_{k^*}$, where x_{k^*} is the nearest constellation point to received signal y , let $\mathbf{c}^{k^*} = (c_0^{k^*} \ c_1^{k^*} \ \dots \ c_{m-1}^{k^*})$ be the binary representation of k^* with the LSB as the rightmost bit. Then, the nearest constellation point to y in subset $\mathcal{X}_i^{(\bar{b}_i^*)}$, namely, $x_{i,\bar{b}_i^*}^*$, can be determined according to

$$x_{i,\bar{b}_i^*}^* = x_{k_i^*} \quad (4)$$

where

$$k_i^* = 2^{m-i-1} - c_i^{k^*} + \sum_{j=0}^{i-1} c_j^{k^*} 2^{m-j-1}. \quad (5)$$

Proof: See Appendix A. ■

- 3) *Calculate L_i according to (2).* After obtaining x^* , \mathbf{b}^* , and $x_{i,\bar{b}_i^*}^*$, we can rewrite L_i as

$$L_i = -\frac{1}{N_0} (1 - 2b_i^*) \left(|y - hx^*|^2 - |y - hx_{i,\bar{b}_i^*}^*|^2 \right). \quad (6)$$

It is clear that (6) is equivalent to (2) for the Gray-labeled PAM. Hence, the performance of the proposed simplified soft demapper is exactly the same as that of the standard Max-Log-MAP demapper, while its complexity is reduced from $O(2^m)$ to $O(m)$.

243 B. QAM Demapper

The 2^m -ary square Gray-labeled QAM can be decomposed into two independent (in-phase and quadrature phase) $2^{m/2}$ -ary Gray-labeled PAMs, and we can apply our proposed simplified PAM demapper to each of these two Gray-labeled PAMs. Thus, the complexity of our simplified Gray-labeled QAM demapper is reduced from $O(2^m)$ to $O(m)$ without suffering any performance loss, in comparison to the standard Max-Log-MAP demapper.

252 C. PSK Demapper

By applying the same idea to PSK demapping, we can also reduce the complexity from $O(2^m)$ to $O(m)$ without any performance loss, compared with the Max-Log-MAP solution. For 2^m -ary Gray-labeled PSK, the signal set can be written in the polar coordinate format as $\mathcal{X} = \{x_k = \sqrt{E_s} \exp(j(2k + 1)\pi/2^m), 0 \leq k < 2^m\}$, where E_s denotes the energy of the transmitted signals, and $j = \sqrt{-1}$. An example of the Gray-8PSK constellation is shown in Fig. 2.

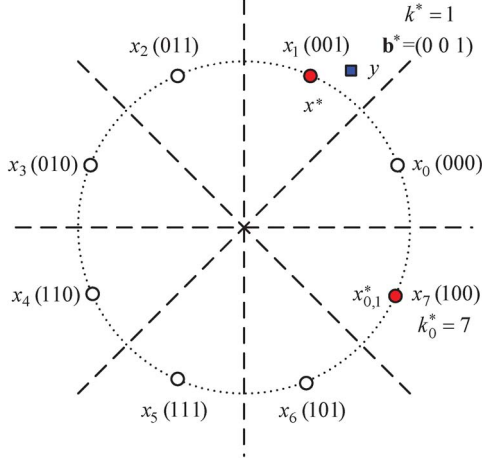


Fig. 2. Gray-8PSK constellation and illustration of demapping for the zeroth bit over the AWGN channel.

Let us express the phase-equalized received signal y in the polar coordinate format as $y = \rho_y \exp(j\varphi_y)$, where ρ_y and φ_y denote the amplitude and phase of y , respectively, and $0 \leq \varphi_y < 2\pi$. Then, the squared Euclidean distance $|y - hx|^2$ can be written as

$$\begin{aligned} |y - hx|^2 &= \left| \rho_y \exp(j\varphi_y) - h\sqrt{E_s} \exp(j\varphi_x) \right|^2 \\ &= \rho_y^2 + h^2 E_s - 2\rho_y h \sqrt{E_s} \cos(\varphi_x - \varphi_y) \\ &= \rho_y^2 + h^2 E_s - 2\rho_y h \sqrt{E_s} \cos(\phi(x, y)) \end{aligned} \quad (7)$$

where φ_x is the phase of x , and $\phi(x, y)$ is defined as

$$\phi(x, y) = \begin{cases} |\varphi_x - \varphi_y|, & 0 \leq |\varphi_x - \varphi_y| \leq \pi \\ 2\pi - |\varphi_x - \varphi_y|, & \pi < |\varphi_x - \varphi_y| < 2\pi \end{cases} \quad (8)$$

It is obvious that $\phi(x, y) \in [0, \pi]$ and is commutative, i.e., $\phi(x, y) = \phi(y, x)$. The mapping defined in (8) also satisfies the triangle inequality, that is, $\forall x, y, z \in \mathbb{C}$, we have

$$\phi(x, z) \leq \phi(x, y) + \phi(y, z) \quad (9)$$

where \mathbb{C} denotes the complex-valued space. The proof is given in Appendix B. Therefore, $\phi(x, y)$ defines a distance over \mathbb{C} , which is referred to as the *phase distance* of x and y in this paper.

Furthermore, multiplying $x \in \mathbb{C}$ with a positive value does not change the phase of x , i.e., $\varphi_{hx} = \varphi_x, \forall h > 0$. Hence, we have $\phi(hx, y) = \phi(x, y), \forall h > 0$. Since the cosine function is a decreasing function in $[0, \pi]$, minimizing the squared Euclidean distance $|y - hx|^2$ of (7) is equivalent to minimizing phase distance $\phi(x, y)$. Therefore, we can simply use the phase of the signal in the search process of the PSK demapper, and the resultant PSK demapping procedure is detailed as follows.

1) *Find x^* and \mathbf{b}^* .* The signal space of the 2^m -ary Gray-labeled PSK can be divided into 2^m phase intervals separated by phase thresholds $0, \pi/2^{m-1}, \dots, (2^m - 1)\pi/2^{m-1}$, as shown in Fig. 2. Signal x^* can be obtained by comparing φ_y with the phase thresholds, which only needs m comparisons using the binary-search algorithm.

Similar to the PAM demapper, after finding $x^* = x_{k^*}$, the corresponding bit vector \mathbf{b}^* is calculated according to Lemma 1. For the case shown in Fig. 2, we have $k^* = 1$ and $\mathbf{b}^* = (0 0 1)$.

2) *Determine $x_{i, \mathbf{b}_i^*}^*$.* Unlike the PAM constellation, the PSK constellation is circularly symmetric, and the phase distance function we used for comparisons is defined in a piecewise fashion. Therefore, calculating $x_{i, \mathbf{b}_i^*}^*$ for the PSK demapper is slightly different from that of the PAM demapper. We have the following lemma for computing $x_{i, \mathbf{b}_i^*}^*$ of Gray-labeled PSK.

Lemma 3: For the binary-reflected Gray PSK $\mathbf{b}^* \rightarrow x_{k^*}$, where x_{k^*} is the constellation point nearest to received signal y , let $\mathbf{c}^{k^*} = (c_0^{k^*} c_1^{k^*} \dots c_{m-1}^{k^*})$ be the binary representation of k^* with the LSB as the rightmost bit. Then, the point nearest to y in subset $\mathcal{X}_i^{(\mathbf{b}_i^*)}$, namely, $x_{i, \mathbf{b}_i^*}^*$, can be determined according to

$$x_{i, \mathbf{b}_i^*}^* = x_{k_i^*} \quad (10)$$

where

$$k_i^* = \begin{cases} c_0^{k^*} 2^{m-1} + c_1^{k^*} (2^{m-1} - 1), & i = 0 \\ 2^{m-i-1} - c_i^{k^*} + \sum_{j=0}^{i-1} c_j^{k^*} 2^{m-j-1}, & i > 0 \end{cases} \quad (11)$$

Proof: See Appendix C. ■

3) *Calculate L_i according to (2).* After obtaining x^*, \mathbf{b}^* , and $x_{i, \mathbf{b}_i^*}^*$, the soft information on the i th bit, i.e., L_i , is calculated according to (6), which is the same result as that in (2) for the Max-Log-MAP demapper, as is the case for the PAM demapper. Clearly, the performance of this simplified soft demapper is identical to that of the Max-Log-MAP demapper, while only imposing a complexity on the order of $O(m)$.

D. Gray-APSK Demapper

1) *Review of Gray-APSK:* A generic M -ary APSK constellation is composed of R concentric rings, each having uniformly spaced PSK points. More specifically, the M -APSK constellation set is given by $\mathcal{X} = \{r_l \exp(j(2\pi i/n_l + \theta_l)), 0 \leq i < n_l, 0 \leq l < R\}$, in which n_l, r_l , and θ_l denote the number of PSK points, the radius, and the phase shift of the l th ring, respectively, while we have $\sum_{l=0}^{R-1} n_l = M$ [21].

In [16], a special APSK constellation was proposed, which consists of $R = 2^{m_2}$ rings and $n_l = 2^{m_1}$ PSK points on each ring for the $(M = 2^m)$ -ary APSK, where we have $m_1 + m_2 = m$. This kind of APSK is known as the product-APSK and is denoted by $(M = 2^{m_1} \times 2^{m_2})$ -APSK. The l th radius of the product-APSK constellation, where $0 \leq l < R$, is determined by

$$r_l = \sqrt{-\ln(1 - (l + 1/2)2^{-m_2})}. \quad (12)$$

The $(2^m = 2^{m_1} \times 2^{m_2})$ -APSK can be regarded as the product of 2^{m_1} -ary PSK and 2^{m_2} -ary pseudo PAM, where the

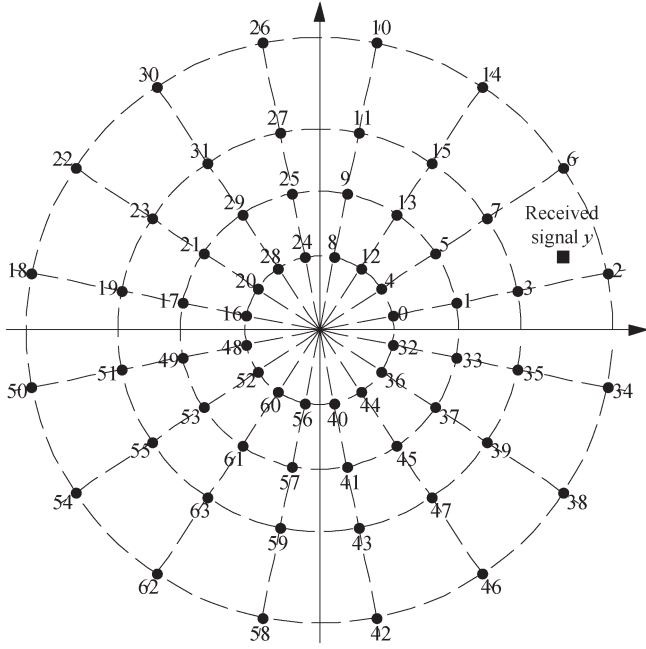


Fig. 3. Gray-labeled (64 = 16 × 4)-APSK constellation, where the labels are in the decimal form with the binary representation having the LSB as the rightmost bit.

332 pseudo PAM and PSK sets are given, respectively, by $\mathcal{A} =$
 333 $\{r_l, 0 \leq l < 2^{m_2}\}$ and $\mathcal{P} = \{p_k = \exp(j\varphi_k) \text{ with } \varphi_k = (2k +$
 334 $1)\pi/2^{m_1}, 0 \leq k < 2^{m_1}\}$ [17]. We divide the m -bit vector
 335 \mathbf{b} into two subvectors \mathbf{b}^P and \mathbf{b}^A of lengths m_1 and m_2 ,
 336 respectively. Specifically, \mathbf{b}^P consists of the leftmost m_1 bits
 337 of \mathbf{b} , whereas \mathbf{b}^A contains the rest rightmost m_2 bits of \mathbf{b} .
 338 Without loss of generality, \mathbf{b}^P is mapped to the equivalent 2^{m_1} -
 339 PSK point, and \mathbf{b}^A is mapped to the equivalent pseudo 2^{m_2} -
 340 PAM point. Gray labeling can be used for mapping the bits to
 341 the equivalent constellation signals. This Gray-labeled APSK
 342 (Gray-APSK) is a special product-APSK [16], [17]. The Gray-
 343 labeled (64 = 16 × 4)-APSK is shown in Fig. 3.

344 2) *Proposed Demapping Algorithm for Gray-APSK*: Like
 345 the other constellations previously discussed, the standard Max-
 346 Log-MAP demapping designed for Gray-APSK also uses (2).
 347 By writing transmitted signal x and received signal y in the
 348 polar-coordinate format, the squared Euclidean distance $|y -$
 349 $hx|^2$ for Gray-APSK can be readily expressed as

$$\begin{aligned} |y - hx|^2 &= \rho_y^2 + h^2 \rho_x^2 - 2h\rho_x\rho_y \cos(\phi(x, y)) \\ &= (\rho_y \cos(\phi(x, y)) - h\rho_x)^2 + \rho_y^2 \sin^2(\phi(x, y)) \end{aligned} \quad (13)$$

350 where ρ_x and ρ_y represent the amplitudes of x and y , respec-
 351 tively, and $\phi(x, y)$ is the phase distance between x and y , as
 352 defined in (8).

353 Due to the circular symmetry of the Gray-APSK constella-
 354 tion, it is clear that the nearest constellation point x^* from y
 355 has the smallest phase distance, i.e., $\phi(x^*, y)$ is the smallest
 356 one in set $\{\phi(x, y), \varphi_x \in \mathcal{P}\}$, and it is no larger than $\pi/2^{m_1}$,
 357 as exemplified in Fig. 3. Furthermore, according to (13), the
 358 amplitude of x^* , which is denoted by ρ_{x^*} , satisfies

$$\rho_{x^*} = \arg \min_{\rho_x \in \mathcal{A}} |\rho_y \cos(\phi(x^*, y)) - h\rho_x|. \quad (14)$$

After determining the phase and the amplitude of x^* , it is easy 359
 to find the corresponding bit label \mathbf{b}^* . As for finding $x_{i, \mathbf{b}_i^*}^*$, this 360
 depends on whether the i th bit is related to the phase or the 361
 amplitude. 362

For the bits related to the phase of the Gray-APSK signal, 363
 i.e., for $0 \leq i < m_1$, the phase of $x_{i, \mathbf{b}_i^*}^*$, which is denoted by 364
 $\varphi_{x_{i, \mathbf{b}_i^*}^*}$, can be readily determined based on Lemma 3 owing to 365
 the uniform distribution of the phases, whereas the amplitude 366
 of $x_{i, \mathbf{b}_i^*}^*$, which is denoted by $\rho_{x_{i, \mathbf{b}_i^*}^*}$, obeys 367

$$\rho_{x_{i, \mathbf{b}_i^*}^*} = \arg \min_{\rho_x \in \mathcal{A}} \left| \rho_y \cos\left(\phi\left(x_{i, \mathbf{b}_i^*}^*, y\right)\right) - h\rho_x \right|. \quad (15)$$

For the bits mapped to the amplitude of the Gray-APSK 368
 signal, i.e., for $m_1 \leq i < m$, it is clear that the phase of $x_{i, \mathbf{b}_i^*}^*$ 369
 is exactly the same as that of x^* , and we may approximately 370
 obtain the amplitude of $x_{i, \mathbf{b}_i^*}^*$ via Lemma 2. However, due to the 371
 nonuniformly spaced amplitudes of \mathcal{A} , such an approximation 372
 may cause some errors, albeit the performance loss is fortu- 373
 nately negligible, as will be detailed later in Section III-D4. 374 AQ1

Upon obtaining x^* , \mathbf{b}^* , and $x_{i, \mathbf{b}_i^*}^*$, we can readily determine 375
 the demapping output of the i th bit based on (6). This simplified 376
 Gray-APSK demapping procedure is summarized as follows. 377

- 1) *Find x^* and \mathbf{b}^** . The phase of x^* is determined by 378
 minimizing the phase difference from y to x with phase 379
 $\varphi_x \in \mathcal{P}$, and its amplitude is determined according to 380
 (14). Having obtained $\varphi_{x^*} = \varphi_{k^*P^*}$ and $\rho_{x^*} = r_{k^*A^*}$, sub- 381
 bit vectors \mathbf{b}^{P^*} and \mathbf{b}^{A^*} are calculated according to 382
 Lemma 1, yielding $\mathbf{b}^* = (\mathbf{b}^{P^*} \mathbf{b}^{A^*})$. 383
- 2) *Determine $x_{i, \mathbf{b}_i^*}^*$* . For the leftmost m_1 bits that are related 384
 to the phases of the Gray-APSK signals, we can obtain 385
 the phase of $x_{i, \mathbf{b}_i^*}^*$ according to Lemma 3 and its amplitude 386
 according to (15). For the rightmost m_2 bits, i.e., $m_1 \leq$ 387
 $i < m$, the phase of $x_{i, \mathbf{b}_i^*}^*$ is exactly the same as φ_{x^*} , and 388
 its amplitude is approximately determined according to 389
 Lemma 2. 390
- 3) *Calculate L_i according to (2)*. After obtaining x^* , \mathbf{b}^* , and 391
 $x_{i, \mathbf{b}_i^*}^*$, the soft information on the i th bit, i.e., L_i , is given 392
 by (6), as for the other demappers. 393

3) *Complexity Analysis*: Step 1) determines x^* and \mathbf{b}^* . The 394
 phase of x^* can be readily obtained by simple comparison 395
 operations, and its amplitude is determined according to (14), 396
 which requires one multiplication for $\rho_y \cos(\phi(x^*, y))$ and 397
 m_2 comparison operations. Having determined x^* , calculating 398
 \mathbf{b}^* only requires some low-complexity XOR operations. The 399
 complexity of step 2) is mainly associated with determining the 400
 amplitude of $x_{i, \mathbf{b}_i^*}^*$ according to (15), for $0 \leq i < m_1$, which 401
 requires one multiplication operation for $\rho_y \cos(\phi(x_{i, \mathbf{b}_i^*}^*, y))$ 402
 and m_2 comparison operations. It is therefore clear that the 403
 complexity of the proposed simplified Gray-APSK demapper 404
 is $O(2 \times m_1 + m_2) \approx O(m)$, which is dramatically lower than 405
 the complexity of $O(2^m)$ required by the standard Max-Log- 406
 MAP solution. 407

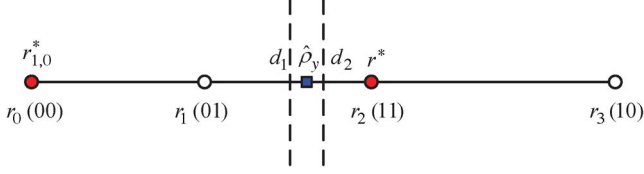


Fig. 4. Pseudo4PAM decomposed from the $(64 = 16 \times 4)$ -APSK constellation.

An alternative complexity analysis, which is “easier” to follow is outlined below. The demapper proposed for $(2^m = 2^{m_1} \times 2^{m_2})$ -APSK is equivalent to the demapper conceived for 2^{m_1} -ary PSK implemented with the aid of the simplified PSK demapping procedure in Section III-C at the complexity of $O(m_1)$ and the demapper for the 2^{m_2} -ary pseudo PAM implemented with the aid of the simplified PAM demapping procedure in Section III-A at the complexity of $O(m_2)$. Therefore, the complexity of the proposed simplified Gray-APSK demapper is approximately $O(m_1) + O(m_2) \approx O(m)$. It is worth emphasizing again that the complexity of our proposed simplified Gray-APSK demapper is also much lower than that of the simplified soft demapper for product-APSK given in [17], which is on the order of $O(2^{m_1}) + O(2^{m_2})$.

4) *Performance Analysis*: Owing to the fact that the phase of the APSK constellation is uniformly spaced, Lemma 3 always holds when demapping the leftmost m_1 bits, and the results of the proposed demapper are exactly the same as those of the Max-Log-MAP demapper. However, unlike in the conventional PAM, the distances between pairs of adjacent points in the corresponding pseudo PAM part of the Gray-APSK constellation are not constant, which means that Lemma 2 does not always hold. Therefore, when demapping the rightmost m_2 bits with the aid of Lemma 2, the resultant x_{i, \bar{b}_i}^* may

not always be the point nearest to y in subset $\mathcal{X}_i^{(\bar{b}_i^*)}$, which may slightly increase the absolute value of the LLR in (2) and, consequently, results in some performance degradation. Fortunately, this degradation is negligible. In the following, we present the detailed analysis of this performance loss with the aid of Gray-labeled 64-APSK and 256-APSK.

a) $(64 = 16 \times 4)$ -APSK: As shown in Fig. 4, to demap the rightmost 2 bits related to the amplitudes in the $(64 = 16 \times 4)$ -APSK, we have the scalar projection of y in the direction of φ_{x^*} and the pseudo Gray 4PAM constellation set \mathcal{A} . We denote the projection as $\hat{\rho}_y = \rho_y \cos(\phi(x^*, y))$ and the thresholds as $d_1 = (r_1 + r_2)/2$ and $d_2 = (r_0 + r_3)/2$. If $\hat{\rho}_y$ is smaller than d_1 , we have $r^* = r_0$ or r_1 , and the zeroth bit of \mathbf{b}^{A^*} must be 0. The constellation subset with the zeroth bit being 1 is $\mathcal{A}_0^{(1)} = \{r_2, r_3\}$, and obviously, the nearest point to $\hat{\rho}_y$ in $\mathcal{A}_0^{(1)}$ is $r_{0,1}^* = r_2$, which is identical to the result given by Lemma 2. If $\hat{\rho}_y$ is larger than d_1 , we have $b_0^{A^*} = 1$ and $r_{0,0}^* = r_1$, which is also the same result given by Lemma 2. Therefore, the proposed demapper achieves the same result as the Max-Log-MAP demapper for the zeroth bit of the pseudo 4PAM, and no error is introduced.

However, for the first bit of the pseudo 4PAM, when $\hat{\rho}_y$ falls in the interval of (d_1, d_2) known as the *error interval*,¹

¹Here, we have $d_1 < d_2$ according to (12).

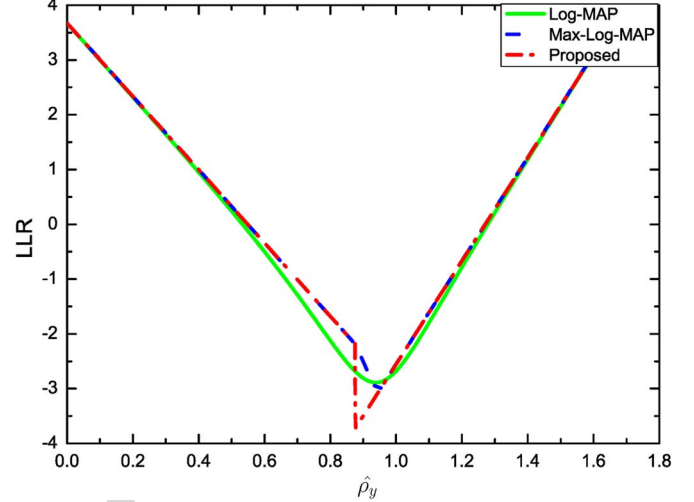


Fig. 5. LLR of the first bit of the pseudo 4PAM decomposed from $(64 = 16 \times 4)$ -APSK over the AWGN channel with $E_s/N_0 = 10$ dB.

the nearest constellation point to $\hat{\rho}_y$ in \mathcal{A} is $r^* = r_2$, and we have $\mathbf{b}^{A^*} = (1 \ 1)$ and $\mathcal{A}_1^{(0)} = \{r_0, r_3\}$. The point nearest to $\hat{\rho}_y$ in $\mathcal{A}_1^{(0)}$ is supposed to be $r_{1,0}^* = r_3$ according to Lemma 2, but in fact, $\hat{\rho}_y$ is closer to r_0 because of the asymmetry of the pseudo PAM. The proposed demapper uses a farther point that increases the absolute value of the LLR in (2). The increment of the absolute value of the LLR caused by the proposed demapper is bounded by

$$\begin{aligned} \Delta L &= (|\hat{\rho}_y - r_3|^2 - |\hat{\rho}_y - r_0|^2) / N_0 \\ &= (r_3 - r_0)(r_0 + r_3 - 2\hat{\rho}_y) / N_0 \\ &< (r_3 - r_0)(r_0 + r_3 - r_1 - r_2) / N_0. \end{aligned} \quad (16)$$

The exact and correct absolute LLR value is

$$\begin{aligned} |L_1| &= (|\hat{\rho}_y - r_0|^2 - |\hat{\rho}_y - r_2|^2) / N_0 \\ &= (r_2 - r_0)(2\hat{\rho}_y - r_0 - r_2) / N_0 \\ &> (r_2 - r_0)(r_1 - r_0) / N_0. \end{aligned} \quad (17)$$

Therefore, the ratio of ΔL over $|L_1|$ is bounded by

$$\frac{\Delta L}{|L_1|} < \frac{(r_3 - r_0)(r_3 + r_0 - r_1 - r_2)}{(r_2 - r_0)(r_1 - r_0)} \approx 0.708. \quad (18)$$

The LLRs of the first bit of the pseudo 4PAM calculated by the Log-MAP, Max-Log-MAP, and our proposed demapper are shown in Fig. 5. The LLR calculated by our proposed demapper is exactly the same as that of the Max-Log-MAP demapper when $\hat{\rho}_y$ is outside the interval (d_1, d_2) . When $d_1 < \hat{\rho}_y < d_2$, the absolute value of the LLR calculated by our proposed demapper is slightly larger than that of the Max-Log-MAP demapper. It is interesting to note that the absolute value of the LLR calculated by the Log-MAP demapper is also slightly larger than that of the Max-Log-MAP demapper in some regions, and it is worth remembering that the Max-Log-MAP solution itself is an approximation of the optimal Log-MAP solution.

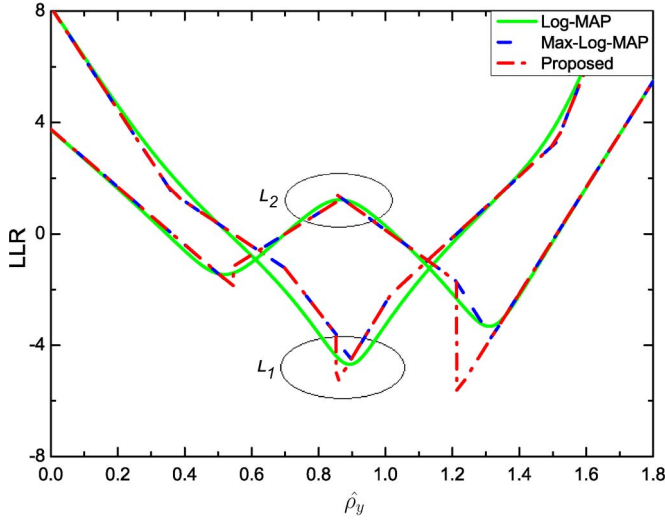


Fig. 6. LLRs of the first and second bits of the pseudo 8PAM decomposed from (256 = 32 × 8)-APSK over the AWGN channel with $E_s/N_0 = 14$ dB.

The ratio (18) associated with the error is an upper bound. Furthermore, this error only exists when $\hat{\rho}_y \in (d_1, d_2)$, which does not frequently happen, as will be detailed later. Before analyzing the probability of $\hat{\rho}_y$ falling into an error interval, we further examine the larger constellation of (256 = 32 × 8)-APSK.

b) (256 = 32 × 8)-APSK: Similar to (64 = 16 × 4)-APSK, for (256 = 32 × 8)-APSK, the error also occurs when demapping the rightmost 3 bits, since we use the pseudo Gray 8PAM constellation. More specifically, if $\hat{\rho}_y$ is smaller than $(r_3 + r_4)/2$, the zeroth bit of \mathbf{b}^{A*} must be 0. The constellation subset associated with the zeroth bit being 1 is $\mathcal{A}_0^{(1)} = \{r_4, r_5, r_6, r_7\}$, and obviously, the point closest to $\hat{\rho}_y$ in $\mathcal{A}_0^{(1)}$ is $r_{0,1}^* = r_4$, which is the same result as that given by Lemma 2. If $\hat{\rho}_y$ is larger than $(r_3 + r_4)/2$, we have $b_0^{A*} = 1$ and $r_{0,0}^* = r_3$, which is also identical to the result given by Lemma 2. Therefore, no error occurs when demapping the zeroth bit using Lemma 2. Demapping the first bit using Lemma 2 has one error interval $((r_3 + r_4)/2, (r_1 + r_6)/2)$, whereas demapping the second bit using Lemma 2 has three error intervals $((r_0 + r_3)/2, (r_1 + r_2)/2)$, $((r_3 + r_4)/2, (r_2 + r_5)/2)$, and $((r_5 + r_6)/2, (r_4 + r_7)/2)$. The LLRs of the first and second bits related to the pseudo 8PAM calculated by the Log-MAP, Max-Log-MAP, and our proposed demapper are shown in Fig. 6. The LLR calculated by our proposed demapper is exactly the same as the Max-Log-MAP demapper when $\hat{\rho}_y$ is outside the error intervals. When $\hat{\rho}_y$ falls within one of the error intervals, the absolute value of the LLR calculated by our proposed demapper is slightly larger than that of the Max-Log-MAP demapper.

3) Error distribution: Since $\phi(x^*, y)$ represents the minimum phase distance between received signal y and the constellation points, we have $\phi(x^*, y) \leq \pi/2^{m_1}$. As the constellation order increases, $\phi(x^*, y)$ tends to 0, and $\cos(\phi(x^*, y))$ tends to 1. For example, in the case of (64 = 16 × 4)-APSK, we have $m_1 = 4$, $\phi(x^*, y) \leq \pi/16 = 0.1963$, and $\cos(\phi(x^*, y)) \geq 0.9808$, whereas in the case of (256 = 32 × 8)-APSK, we have $m_1 = 5$, $\phi(x^*, y) \leq \pi/32 = 0.0982$, and $\cos(\phi(x^*, y)) \geq$

0.9952. Then, $\hat{\rho}_y$ can be approximated by ρ_y , which obeys a Rician distribution. Specifically

$$p(\hat{\rho}_y|r) \approx \frac{2\hat{\rho}_y}{N_0} \exp\left(-\frac{\hat{\rho}_y^2 + r^2}{N_0}\right) I_0\left(\frac{2r\hat{\rho}_y}{N_0}\right) \quad (19)$$

where r denotes the amplitude of transmitted signal x , and $I_0(\cdot)$ is the modified Bessel function of the first kind with order zero.

The error intervals for the 2^{m_2} -ary pseudo PAM can be determined in the following recursive way.

- i) For the zeroth bit and $m_2 \geq 1$, there is no error interval.
- ii) For the first bit and $m_2 = 2$, the error interval is $((r_1 + r_2)/2, (r_0 + r_3)/2)$.
- iii) For the k th bit, where $1 \leq k < m_2$ and $m_2 \geq 2$, there are $2^k - 1$ error intervals. We denote the i th error interval as $(d_{i,1}^{m_2,k}, d_{i,2}^{m_2,k})$, where

$$d_{i,1}^{m_2,k} = \min\left\{\left(r_{e_{i,1}^{m_2,k}} + r_{e_{i,2}^{m_2,k}}\right)/2, \left(r_{e_{i,3}^{m_2,k}} + r_{e_{i,4}^{m_2,k}}\right)/2\right\} \quad (20)$$

$$d_{i,2}^{m_2,k} = \max\left\{\left(r_{e_{i,1}^{m_2,k}} + r_{e_{i,2}^{m_2,k}}\right)/2, \left(r_{e_{i,3}^{m_2,k}} + r_{e_{i,4}^{m_2,k}}\right)/2\right\} \quad (21)$$

and $e_{i,j}^{m_2,k}$ denotes the index of the corresponding radius calculated by (12). For example, for case ii), we have $e_{1,1}^{2,1} = 1$, $e_{1,2}^{2,1} = 2$, $e_{1,3}^{2,1} = 0$, and $e_{1,4}^{2,1} = 3$. In general, index $e_{i,j}^{m_2,k}$ can be recursively determined from $e_{i,j}^{m_2-1,k-1}$ according to

$$e_{i,j}^{m_2,k} = \begin{cases} e_{i,j}^{m_2-1,k-1}, & 1 \leq i \leq 2^{k-1} - 1 \\ 2^{m_2} - 1 - e_{i,j}^{m_2-1,k-1}, & 1 \leq j \leq 4 \\ & 2^{k-1} \leq i < 2^k - 1 \\ 2^{m_2-1} - 1, & 1 \leq j \leq 4 \\ & i = 2^k - 1; j = 1 \\ 2^{m_2-1}, & i = 2^k - 1; j = 2 \\ 2^{m_2-1} - 2^{m_2-k-1} - 1, & i = 2^k - 1; j = 3 \\ 2^{m_2-1} + 2^{m_2-k-1}, & i = 2^k - 1; j = 4. \end{cases} \quad (22)$$

For the product-APSK constellation set \mathcal{X} , each ring has the same number of points, and radius r is uniformly distributed over set \mathcal{A} . Therefore, the probability of $\hat{\rho}_y$ falling into the error interval $(d_{i,1}^{m_2,k}, d_{i,2}^{m_2,k})$ is readily shown to be

$$\begin{aligned} P\left(d_{i,1}^{m_2,k} < \hat{\rho}_y < d_{i,2}^{m_2,k}\right) &= \sum_{s=0}^{2^{m_2}-1} P(r_s) P\left(d_{i,1}^{m_2,k} < \hat{\rho}_y < d_{i,2}^{m_2,k} | r_s\right) \\ &= \frac{1}{2^{m_2}} \sum_{s=0}^{2^{m_2}-1} \int_{d_{i,1}^{m_2,k}}^{d_{i,2}^{m_2,k}} p(\hat{\rho}_y|r_s) d\hat{\rho}_y. \end{aligned} \quad (23)$$

It is clear that (23) does not have a closed-form expression. Fortunately, since the Rician distribution can be approximated by the Gaussian distribution at a high SNR, we have

$$\begin{aligned} P\left(d_{i,1}^{m_2,k} < \hat{\rho}_y < d_{i,2}^{m_2,k}\right) &\approx \frac{1}{2^{m_2}} \sum_{s=0}^{2^{m_2}-1} \left(Q\left(\frac{d_{i,1}^{m_2,k} - r_s}{\sqrt{N_0/2}}\right) - Q\left(\frac{d_{i,2}^{m_2,k} - r_s}{\sqrt{N_0/2}}\right) \right) \end{aligned} \quad (24)$$

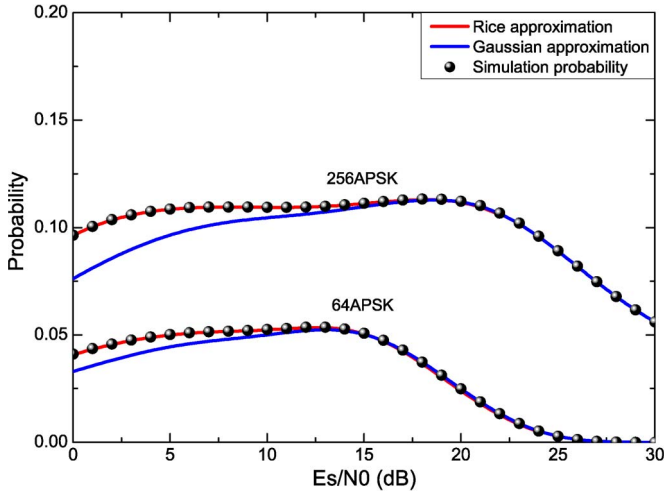


Fig. 7. Probability of $\hat{\rho}_y$ falling into the error interval(s) for $(64 = 16 \times 4)$ -APSK and $(256 = 32 \times 8)$ -APSK, for the AWGN channel.

and the probability of $\hat{\rho}_y$ falling into the error intervals can be obtained by

$$P_e \approx \frac{1}{2^{m_2}} \times \sum_{s=0}^{2^{m_2}-1} \sum_{k=1}^{m_2-1} \sum_{i=1}^{2^k-1} \left(Q\left(\frac{d_{i,1}^{m_2,k} - r_s}{\sqrt{N_0/2}}\right) - Q\left(\frac{d_{i,2}^{m_2,k} - r_s}{\sqrt{N_0/2}}\right) \right) \quad (25)$$

where $Q(x) = (1/\sqrt{2\pi}) \int_x^\infty \exp(-u^2/2) du$ represents the standard tail probability function of the Gaussian distribution with zero mean and unity variance.

For the case of $(64 = 16 \times 4)$ -APSK, the probability of $\hat{\rho}_y$ falling into the error interval is shown in Fig. 7, as the function of the SNR = E_s/N_0 over the AWGN channel. Three P_e 's are shown in Fig. 7, namely, the two theoretical P_e 's derived by the Rician and Gaussian approximations and the probability P_e obtained by simulation. It can be observed that the probability of $\hat{\rho}_y$ falling into the error interval is quite small even at low SNRs. At high SNRs, the Gaussian approximation matches well with the simulation result, and probability P_e tends to zero with the increase in the SNR. This is due to the fact that received signal y is likely to be very close to transmitted signal x at a high SNR, and consequently, the probability of $\hat{\rho}_y$ falling into the error interval becomes extremely small.

Fig. 7 also shows the probability of $\hat{\rho}_y$ falling into the error intervals for $(256 = 32 \times 8)$ -APSK for transmission over the AWGN channel at different SNR values. Probability P_e is much higher than that of 64-APSK, since 256-APSK has more error intervals, but it is no more than 12% at low SNRs. At high SNRs, the Gaussian approximation matches well with the simulation result, and the probability decreases with the increase in the SNR. Probability P_e tends to zero, given a sufficiently high SNR value, which is outside the SNR region shown in Fig. 7.

Our theoretical analysis of $(64 = 16 \times 4)$ -APSK and $(256 = 32 \times 8)$ -APSK, therefore, shows that the error caused by the proposed simplified demapper is relatively small compared

with the accurate LLR, and the probability of $\hat{\rho}_y$ falling into the error intervals is also small (less than 6% for 64-APSK and less than 12% for 256-APSK). Moreover, probability P_e tends to zero at a sufficiently high SNR value. We can conclude that the performance degradation associated with the proposed demapper is negligible for $(64 = 16 \times 4)$ -APSK and $(256 = 32 \times 8)$ -APSK, in comparison with that of the Max-Log-MAP demapper. This will be further demonstrated by the bit error rate (BER) simulation results in Section IV.

It should be noted that Lemma 2 and 3 can be implemented with the aid of a lookup table that defines the interval of y and identifies which particular k_i^* is used for each of the intervals specified by a set of thresholds. For nonuniform constellations such as product-APSK, we can use a larger lookup table, which contains the additional error intervals required for maintaining the performance, albeit this requires more comparison operations and an increased storage capacity.

IV. SIMULATION RESULTS

The BER performance of the proposed soft demapper was evaluated by simulation. According to our analysis presented in the previous sections, the proposed soft demapper achieves exactly the same performance as the standard Max-Log-MAP demapper for Gray-labeled PAM, PSK, and QAM. By contrast, it suffers from a slight performance loss for the Gray-labeled product-APSK because of the nonuniformly spaced pseudo PAM constellation embedded in the product-APSK. We therefore carried out simulations for the QAM and product-APSK constellations. The simulation parameters are listed as follows.

- Constellation Labeling: gray-labeled 64QAM, $(64 = 16 \times 4)$ -APSK, 256QAM and $(256 = 32 \times 8)$ -APSK;
- Demapper: the standard Max-Log-MAP demapper and the proposed simplified soft demapper;
- Decoder: the 1/2-rate 64 800-bit long low-density parity-check (LDPC) code of DVB-T2 was employed, whereby the normalized Min-Sum decoding algorithm with a normalization factor of $\alpha = 1/0.875$ was selected [22]. The maximum number of LDPC iterations was set to 50;
- Channel: AWGN and independent identically distributed Rayleigh fading channels.

The achievable BER performance is shown in Figs. 8 and 9 for the AWGN and Rayleigh fading channels, respectively. It can be observed that the BER curves obtained by the Max-Log-MAP and our simplified demappers are overlapped for the Gray-labeled 64QAM and 256QAM over both the AWGN and Rayleigh fading channels. This confirms that the soft information calculated by our proposed demapper is exactly the same as that of the Max-Log-MAP demapper. The results shown in Figs. 8 and 9 also confirm that for the Gray-labeled product-APSK, the performance degradation caused by the proposed demapper is negligible compared with the Max-Log-MAP demapper. Specifically, at the BER of 10^{-5} , the performance loss is below 0.05 dB for the Gray-labeled 64APSK and 256APSK over both AWGN and Rayleigh channels, as shown in Figs. 8 and 9. As expected, the performance degradation in the case of $(256 = 32 \times 8)$ -APSK is slightly higher than that of the $(64 = 16 \times 4)$ -APSK, owing to the fact that 256APSK

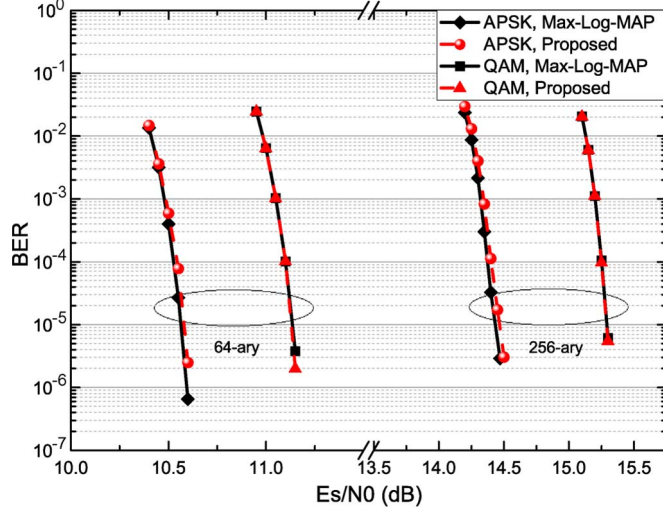


Fig. 8. BER performance comparison over the AWGN channel.

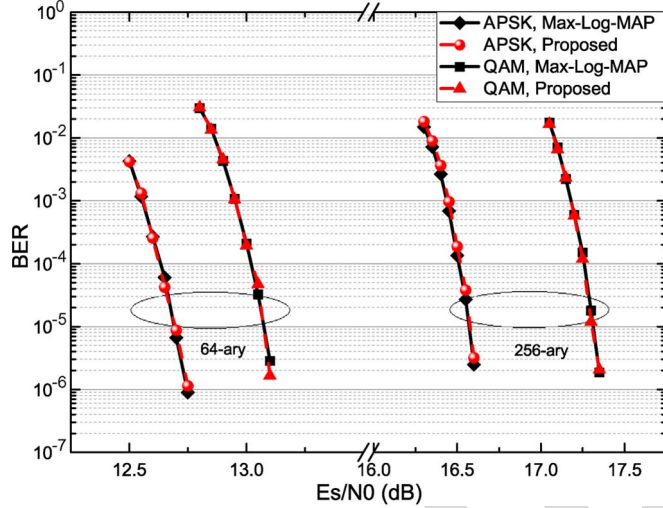


Fig. 9. BER performance comparison over the Rayleigh fading channel.

627 has one more bit related to the pseudo PAM. However, the
628 performance loss still remains below 0.05 dB for 256APSK.

629

V. CONCLUSION

630 In this paper, a universal simplified soft demapper has been
631 proposed for various binary-reflected Gray-labeled constella-
632 tions. For the constellation of size 2^m , our proposed demap-
633 per imposes a low-complexity order of $O(m)$, instead of the
634 complexity order of $O(2^m)$ imposed by the standard Max-Log-
635 MAP demapper. Our theoretical analysis and simulation results
636 have shown that the proposed simplified demapper achieves
637 exactly the same performance as that of the Max-Log-MAP
638 solution for Gray-labeled PAM, PSK, and QAM, whereas for
639 the Gray-labeled product-APSK, the performance degradation
640 caused by our simplified demapper remains negligible com-
641 pared with that of the Max-Log-MAP demapper. More particu-
642 larly, we have verified that this performance loss is less than
643 0.05 dB for both (64 = 16 × 4)-APSK and (256 = 32 × 8)-
644 APSK for transmission over both the AWGN and Rayleigh
645 fading channels.

APPENDIX A

PROOF OF LEMMA 2

646 Once x^* and \mathbf{b}^* are determined, constellation subset $\mathcal{X}_i^{(\bar{b}_i^*)}$ 648
649 can be written as

$$\mathcal{X}_i^{(\bar{b}_i^*)} = \{x_k | x_k \in \mathcal{X}, c_{i-1}^k \oplus c_i^k = \bar{b}_i^*\} \quad (26)$$

where $\mathbf{c}^k = (c_0^k c_1^k \dots c_{m-1}^k)$ denotes the binary representation 650
of k , and we have $c_{-1}^k = 0$. By denoting the nearest constella- 651
tion point to x^* in subset $\mathcal{X}_i^{(\bar{b}_i^*)}$ as the k_i^* th constellation point 652
 $x_{k_i^*}$, we have 653

$$x_{k_i^*} = \arg \min_{x \in \mathcal{X}_i^{(\bar{b}_i^*)}} |x^* - x| \quad (27)$$

$$k_i^* = \arg \min_{k \in \mathcal{K}_i^{(\bar{b}_i^*)}} |k^* - k| \quad (28)$$

where $\mathcal{K}_i^{(\bar{b}_i^*)} = \{k | 0 \leq k < 2^m, c_{i-1}^k \oplus c_i^k = \bar{b}_i^*\}$ denotes the 654
index set corresponding to $\mathcal{X}_i^{(\bar{b}_i^*)}$. 655

For $k \in \mathcal{K}_i^{(\bar{b}_i^*)}$, we can express k as $k = \sum_{j=0}^{m-1} c_j^k 2^{m-j-1}$, 656
where we have $c_{i-1}^k \oplus c_i^k = \bar{b}_i^* = \bar{c}_{i-1}^{k^*} \oplus c_i^{k^*}$. Therefore, 657
we have 658

$$c_{i-1}^k = \bar{c}_{i-1}^{k^*} \text{ and } c_i^k = c_i^{k^*} \text{ or } c_{i-1}^k = c_{i-1}^{k^*} \text{ and } c_i^k = \bar{c}_i^{k^*}. \quad (29)$$

We now discuss the two situations. 659

i) The case of $c_{i-1}^k = \bar{c}_{i-1}^{k^*}$ and $c_i^k = c_i^{k^*}$. We have $c_{i-1}^{k^*} - 660$
 $c_{i-1}^k = \pm 1$, and 661

$$\begin{aligned} & \left| \sum_{j_1=0}^{i-2} (c_{j_1}^{k^*} - c_{j_1}^k) 2^{m-j_1-1} + (c_{i-1}^{k^*} - c_{i-1}^k) 2^{m-i} \right| \\ &= 2^{m-i} \left| \sum_{j_1=0}^{i-2} (c_{j_1}^{k^*} - c_{j_1}^k) 2^{i-j_1-1} + (c_{i-1}^{k^*} - c_{i-1}^k) \right| \\ &\geq 2^{m-i} \quad (30) \end{aligned}$$

where the inequality follows from the fact that 662
 $\sum_{j_1=0}^{i-2} (c_{j_1}^{k^*} - c_{j_1}^k) 2^{i-j_1-1}$ must be even and that 663
 $c_{i-1}^{k^*} - c_{i-1}^k$ is odd. We also have 664

$$\begin{aligned} & \left| \sum_{j_2=i+1}^{m-1} (c_{j_2}^{k^*} - c_{j_2}^k) 2^{m-j_2-1} \right| \leq \sum_{j_2=i+1}^{m-1} |c_{j_2}^{k^*} - c_{j_2}^k| 2^{m-j_2-1} \\ &\leq \sum_{j_2=i+1}^{m-1} 2^{m-j_2-1} = 2^{m-i-1} - 1. \quad (31) \end{aligned}$$

Then, we can find the lower bound of $|k^* - k|$ as 665

$$\begin{aligned} |k^* - k| &= \left| \sum_{j_1=0}^{i-2} (c_{j_1}^{k^*} - c_{j_1}^k) 2^{m-j_1-1} + (c_{i-1}^{k^*} - c_{i-1}^k) 2^{m-i} \right. \\ &\quad \left. + \sum_{j_2=i+1}^{m-1} (c_{j_2}^{k^*} - c_{j_2}^k) 2^{m-j_2-1} \right| \\ &\geq |2^{m-i} - (2^{m-i-1} - 1)| = 2^{m-i-1} + 1. \quad (32) \end{aligned}$$

666 ii) The case of $c_{i-1}^k = c_{i-1}^{k^*}$ and $c_i^k = \overline{c_i^{k^*}}$. If $\exists j_1 \in$
 667 $\{0, 1, \dots, i-2\}$, which makes $c_{j_1}^k \neq c_{j_1}^{k^*}$, then we have

$$\begin{aligned} |k^* - k| &= \left| \sum_{j_1=0}^{i-2} (c_{j_1}^{k^*} - c_{j_1}^k) 2^{m-j_1-1} \right. \\ &\quad \left. + \sum_{j_2=i}^{m-1} (c_{j_2}^{k^*} - c_{j_2}^k) 2^{m-j_2-1} \right| \\ &\geq \left| \sum_{j_1=0}^{i-2} (c_{j_1}^{k^*} - c_{j_1}^k) 2^{m-j_1-1} \right| \\ &\quad - \left| \sum_{j_2=i}^{m-1} (c_{j_2}^{k^*} - c_{j_2}^k) 2^{m-j_2-1} \right| \\ &\geq |2^{m-i+1} - (2^{m-i} - 1)| = 2^{m-i} + 1. \end{aligned} \quad (33)$$

668 On the other hand, if $c_{j_1}^k = c_{j_1}^{k^*}$ for $0 \leq j_1 \leq i-2$,
 669 we have

$$\begin{aligned} |k^* - k| &= \left| \left(c_i^{k^*} - \overline{c_i^{k^*}} \right) 2^{m-i-1} + \sum_{j_2=i+1}^{m-1} (c_{j_2}^{k^*} - c_{j_2}^k) 2^{m-j_2-1} \right| \\ &= 2^{m-i-1} - (-1)^{c_i^{k^*}} \sum_{j_2=i+1}^{m-1} c_{j_2}^{k^*} 2^{m-j_2-1} \\ &\quad + (-1)^{c_i^{k^*}} \sum_{j_2=i+1}^{m-1} c_{j_2}^k 2^{m-j_2-1}. \end{aligned} \quad (34)$$

670 Apparently, the minimum of (34) is smaller than 2^{m-i-1} and,
 671 thus, smaller than both the lower bounds given in (32) and (33).
 672 Since the first two items in (34) are fixed, minimizing $|k^* -$
 673 $k|$ is equivalent to minimizing $(-1)^{c_i^{k^*}} \sum_{j_2=i+1}^{m-1} c_{j_2}^{k^*} 2^{m-j_2-1}$.
 674 Therefore, we have $c_j^{k^*} = c_i^{k^*}$, $i+1 \leq j \leq m-1$, and

$$\begin{aligned} k_i^* &= \sum_{j_1=0}^{i-2} c_{j_1}^{k^*} 2^{m-j_1-1} + \overline{c_i^{k^*}} 2^{m-i-1} + \sum_{j_2=i+1}^{m-1} c_{j_2}^{k^*} 2^{m-j_2-1} \\ &= 2^{m-i-1} - c_i^{k^*} + \sum_{j=0}^{i-1} c_j^{k^*} 2^{m-j-1}. \end{aligned} \quad (35)$$

675 It is clear that k_i^* is the unique solution of (28). Hence, $\forall k \in$
 676 $\mathcal{K}_i^{(\overline{b_i^*})} \setminus \{k_i^*\}$, we have $|k^* - k| \geq |k^* - k_i^*| + 1$, and

$$|x^* - x_k| \geq |x^* - x_{k_i^*}| + \delta. \quad (36)$$

677 Since x^* is the nearest constellation point to y , we obtain

$$|y - hx^*| \leq |h|\delta/2 \quad (37)$$

for $y \in [-2^{m-1}|h|\delta, 2^{m-1}|h|\delta]$. In this case, for $k \in \mathcal{K}_i^{(\overline{b_i^*})} \setminus$
 678 $\{k_i^*\}$, we have 679

$$\begin{aligned} |y - hx_k| &\geq |h(x^* - x_k)| - |y - hx^*| \\ &\geq |h|(|x^* - x_{k_i^*}| + \delta) - |h|\delta/2 \\ &\geq |h(x^* - x_{k_i^*})| + |y - hx^*| \geq |y - hx_{k_i^*}|. \end{aligned} \quad (38)$$

It is easy to find that this inequality still holds when y is outside
 680 the interval $[-2^{m-1}|h|\delta, 2^{m-1}|h|\delta]$. Therefore, $x_{k_i^*}$ is not only
 681 the nearest constellation point to x^* in $\mathcal{X}_i^{(\overline{b_i^*})}$ but the nearest
 682 constellation point to y in $\mathcal{X}_i^{(\overline{b_i^*})}$ as well. This completes the
 683 proof of Lemma 2. ■ 684

APPENDIX B

PROOF OF THE TRIANGLE INEQUALITY OF THE PHASE DISTANCE

From (8), $\phi(x, y)$ can be rewritten as $\phi(x, y) = \min\{|\varphi_x -$
 688 $\varphi_y|, 2\pi - |\varphi_x - \varphi_y|\}$. The proof is divided into three parts
 689 according to the values of $|\varphi_x - \varphi_y|$ and $|\varphi_y - \varphi_z|$. 690

i) If $|\varphi_x - \varphi_y| \leq \pi$ and $|\varphi_y - \varphi_z| \leq \pi$, we have 691

$$\phi(x, y) + \phi(y, z) = |\varphi_x - \varphi_y| + |\varphi_y - \varphi_z| \geq |\varphi_x - \varphi_z| \geq \phi(x, z). \quad (39)$$

ii) For $|\varphi_x - \varphi_y| > \pi$ and $|\varphi_y - \varphi_z| \leq \pi$ or $|\varphi_x - \varphi_y| \leq \pi$
 692 and $|\varphi_y - \varphi_z| > \pi$, without loss of generality, we assume
 693 $|\varphi_x - \varphi_y| > \pi$ and $|\varphi_y - \varphi_z| \leq \pi$. Then, we have 694

$$\begin{aligned} \phi(x, y) + \phi(y, z) &= 2\pi - |\varphi_x - \varphi_y| + |\varphi_y - \varphi_z| \\ &\geq 2\pi - |\varphi_x - \varphi_z| \geq \phi(x, z). \end{aligned} \quad (40)$$

iii) For $|\varphi_x - \varphi_y| > \pi$ and $|\varphi_y - \varphi_z| > \pi$, without loss of
 695 generality, we assume $\varphi_x \geq \varphi_z$. Since φ_x, φ_y , and φ_z are
 696 all inside the interval $[0, 2\pi]$, we have $\varphi_x \geq \varphi_z > \varphi_y + \pi$
 697 or $\varphi_z \leq \varphi_x < \varphi_y - \pi$. If $\varphi_x \geq \varphi_z > \varphi_y + \pi$, we have 698

$$|\varphi_x - \varphi_y| + |\varphi_y - \varphi_z| + |\varphi_x - \varphi_z| = 2\varphi_x - 2\varphi_y < 4\pi. \quad (41)$$

If $\varphi_z \leq \varphi_x < \varphi_y - \pi$, we have 699

$$|\varphi_x - \varphi_y| + |\varphi_y - \varphi_z| + |\varphi_x - \varphi_z| = 2\varphi_y - 2\varphi_z < 4\pi. \quad (42)$$

In both cases, we have 700

$$\begin{aligned} \phi(x, y) + \phi(y, z) &= 2\pi - |\varphi_x - \varphi_y| + 2\pi - |\varphi_y - \varphi_z| > |\varphi_x - \varphi_z| \\ &\geq \phi(x, z). \end{aligned} \quad (43)$$

This completes the proof. ■ 701

APPENDIX C

PROOF OF LEMMA 3

The definitions of $\mathcal{X}_i^{(\overline{b_i^*})}$ and $x_{k_i^*}$ are the same as given in
 704 (26) and (27). Noting that 705

$$\begin{aligned} |x^* - x|^2 &= \left| \sqrt{E_s} \exp(j\varphi_{x^*}) - \sqrt{E_s} \exp(j\varphi_x) \right|^2 \\ &= 2E_s - 2E_s \cos(\phi(x^*, x)) \end{aligned} \quad (44)$$

706 we have

$$k_i^* = \arg \min_{k \in \mathcal{K}_i^{(\bar{b}_i^*)}} \phi(x_k^*, x_k). \quad (45)$$

707 Similar to the proof of Lemma 2, we can get the unique solution
708 of k_i^* as shown in (11), which means that $\forall k \in \mathcal{K}_i^{(\bar{b}_i^*)} \setminus \{k_i^*\}$,
709 we have

$$\phi(x_k, x^*) \geq \phi(x^*, x_{k_i^*}) + 2\pi/2^m. \quad (46)$$

710 Since x^* is the nearest constellation point to y , we obtain

$$\phi(x^*, y) \leq \pi/2^m. \quad (47)$$

711 According to (7), (9), (46), and (47), we have, $\forall k \in \mathcal{K}_i^{(\bar{b}_i^*)} \setminus \{k_i^*\}$

$$\begin{aligned} \phi(x_k, y) &\geq \phi(x^*, x_k) - \phi(x^*, y) \\ &\geq \phi(x^*, x_{k_i^*}) + 2\pi/2^m - \pi/2^m \\ &\geq \phi(x^*, x_{k_i^*}) + \phi(x^*, y) \geq \phi(x_{k_i^*}, y) \end{aligned} \quad (48)$$

$$|y - hx_k| \geq |y - hx_{k_i^*}|. \quad (49)$$

712 Therefore, $x_{k_i^*}$ is not only the nearest constellation point to x^*
713 in $\mathcal{X}_i^{(\bar{b}_i^*)}$ but the nearest constellation point to y in $\mathcal{X}_i^{(\bar{b}_i^*)}$ as well.
714 This completes the proof. ■

REFERENCES

- 716 [1] *Digital Video Broadcasting (DVB); Frame Structure Channel Coding and*
717 *Modulation for a Second Generation Digital Terrestrial Television Broad-*
718 *casting System (DVB-T2)*, ETSI EN Std. 302 755 V1.3.1, Apr. 2012.
- 719 [2] *Digital Video Broadcasting (DVB); Frame Structure Channel Coding and*
720 *Modulation for a Second Generation Digital Transmission System for*
721 *Cable Systems (DVB-C2)*, ETSI EN Std. 302 769 V1.2.1, Apr. 2012.
- 722 [3] Third-Generation Partnership Project (3GPP); Technical specification
723 group radio access network; Physical layer aspects for evolved UTRA,
724 Third-Generation Partnership Project (3GPP), Sophia Antipolis, France.
725 [Online]. Available: <http://www.3gpp.org/ftp/Specs/html-info/25814.htm>
- 726 [4] J. Erfanian, S. Pasupathy, and G. Gulak, "Reduced complexity symbol de-
727 tectors with parallel structures for ISI channels," *IEEE Trans. Commun.*,
728 vol. 42, no. 2/3/4, pp. 1661–1671, Feb./Mar./Apr. 1994.
- 729 [5] P. Robertson, E. Villebrun, and P. Hoeher, "A comparison of optimal
730 and sub-optimal MAP decoding algorithms operating in the log domain,"
731 in *Proc. IEEE ICC*, Seattle, WA, USA, Jun. 18–22, 1995, vol. 2,
732 pp. 1009–1013.
- 733 [6] L. Wang, D. Xu, and X. Zhang, "Recursive bit metric generation for PSK
734 signals with Gray labeling," *IEEE Commun. Lett.*, vol. 16, no. 2, pp. 180–
735 182, Feb. 2012.
- 736 [7] E. Akay and E. Ayanoglu, "Low complexity decoding of bit-interleaved
737 coded modulation for M-ary QAM," in *Proc. IEEE ICC*, Paris, France,
738 Jun. 20–24, 2004, vol. 2, pp. 901–905.
- 739 [8] C.-W. Chang, P.-N. Chen, and Y. S. Han, "A systematic bit-wise decom-
740 position of M-ary symbol metric," *IEEE Trans. Wireless Commun.*, vol. 5,
741 no. 10, pp. 2742–2751, Oct. 2006.
- 742 [9] F. Tosato and P. Bisaglia, "Simplified soft-output demapper for binary
743 interleaved COFDM with application to HIPERLAN/2," in *Proc. IEEE*
744 *ICC*, New York, NY, USA, Apr. 28/May 2, 2002, vol. 2, pp. 664–668.
- 745 [10] M. Zhang and S. Kim, "Efficient soft demapping for M-ary APSK," in
746 *Proc. ICTC*, Seoul, Korea, Sep. 28–30, 2011, pp. 641–644.
- 747 [11] G. Gül, A. Vargas, W. H. Gerstacker, and M. Breiling, "Low complex-
748 ity demapping algorithms for multilevel codes," *IEEE Trans. Commun.*,
749 vol. 59, no. 4, pp. 998–1008, Apr. 2011.
- 750 [12] J. W. Park, M. H. Sunwoo, P. S. Kim, and D.-I. Chang, "Low complexity
751 soft-decision demapper for high order modulation of DVB-S2 system," in
752 *Proc. ISOCC*, Busan, Korea, Nov. 24, 2008, pp. II-37–II-40.
- 753 [13] D. Pérez-Calderón, V. Baena-Lecuyer, A. C. Oria, P. López, and
754 J. G. Doblado, "Rotated constellation demapper for DVB-T2," *Electron.*
755 *Lett.*, vol. 47, no. 1, pp. 31–32, Jan. 2011.
- 756 [14] S. Tomasin and M. Butussi, "Low complexity demapping of rotated and
757 cyclic Q delayed constellations for DVB-T2," *IEEE Wireless Commun.*
758 *Lett.*, vol. 1, no. 2, pp. 81–84, Apr. 2012.

- [15] Y. Fan and C. Tsui, "Low-complexity rotated QAM demapper for the
iterative receiver targeting DVB-T2 standard," in *Proc. IEEE VTC-Fall*,
Québec City, QC, Canada, Sep. 3–6, 2012, pp. 1–5.
- [16] Z. Liu, Q. Xie, K. Peng, and Z. Yang, "APSK constellation with
Gray mapping," *IEEE Commun. Lett.*, vol. 15, no. 12, pp. 1271–1273,
Dec. 2011.
- [17] Q. Xie, Z. Wang, and Z. Yang, "Simplified soft demapper for APSK with
product constellation labeling," *IEEE Trans. Wireless Commun.*, vol. 11,
no. 7, pp. 2649–2657, Jul. 2012.
- [18] F. Gray, "Pulse code communications," US Patent 2632058, Mar. 17,
1953.
- [19] E. Agrell, J. Lassing, E. G. Ström, and T. Ottosson, "On the optimality of
the binary reflected Gray code," *IEEE Trans. Inf. Theory*, vol. 50, no. 12,
pp. 3170–3182, Dec. 2004.
- [20] E. M. Reingold, J. Nievergelt, and N. Deo, *Combinatorial Algorithms: The-
ory and Practice*. Englewood Cliffs, NJ, USA: Prentice-Hall, 1977.
- [21] R. De Gaudenzi, A. Guillen, and A. Martinez, "Performance analysis of
turbo-coded APSK modulations over nonlinear satellite channels," *IEEE*
Trans. Wireless Commun., vol. 5, no. 9, pp. 2396–2407, Sep. 2006.
- [22] J. Chen and M. P. C. Fossorier, "Near optimum universal belief propa-
gation based decoding of low-density parity check codes," *IEEE Trans.*
Commun., vol. 50, no. 3, pp. 406–414, Mar. 2002.



Qi Wang received the B.S. degree from Tsinghua University, Beijing, China, in 2011, where he is currently working toward the Ph.D. degree with the Department of Electronic Engineering. His current research interests include optical wireless communications and channel coding and modulation.



Qiuliang Xie received the B.Eng. degree in telecommunication engineering from Beijing University of Posts and Telecommunications, Beijing, China, in 2006 and the Ph.D. degree in electronic engineering from Tsinghua University, Beijing, in 2011, both with high honors.

From July 2011 to March 2013, he was with Digital TV National Engineering Laboratory (Beijing) Co., Ltd., where he participated in developing China's next-generation broadcasting standard. He is currently a Postdoctoral Fellow with the Department

of Radiation Oncology, University of California, Los Angeles, CA, USA, where he is engaged in medical image processing. His main research interests include medical image processing and broadband wireless communication, specially including information theory, coding theory, and image/signal processing theories.

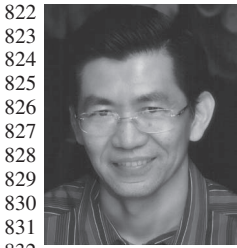


Zhaocheng Wang (SM'10) received the B.S., M.S., and Ph.D. degrees from Tsinghua University, Beijing, China, in 1991, 1993, and 1996, respectively.

From 1996 to 1997, he was a Postdoctoral Fellow with Nanyang Technological University, Singapore. From 1997 to 1999, he was with OKI Techno Centre (Singapore) Pte. Ltd., first as a Research Engineer and then as a Senior Engineer. From 1999 to 2009, he was with Sony Deutschland GmbH, first as a Senior Engineer and then as a Principal Engineer. He is

currently a Professor with the Department of Electronic Engineering, Tsinghua University. He has published over 80 technical papers. He is the holder of 30 U.S./European Union patents. His research interests include wireless communications, digital broadcasting, and millimeter-wave communications.

Dr. Wang has served as a Technical Program Committee Cochair/Member of many international conferences. He is a Fellow of the Institution of Engineering and Technology.



Sheng Chen (M'90–SM'97–F'08) received the B.Eng. degree in control engineering from East China Petroleum Institute, Dongying, China, in 1982; the Ph.D. degree in control engineering from City University London, London, U.K., in 1986; and the D.Sc. degree from the University of Southampton, Southampton, U.K., in 2005.

From 1986 to 1999, he held research and academic appointments with The University of Sheffield, The University of Edinburgh, and the University of Portsmouth, all in the U.K. Since 1999, he has been

with Electronics and Computer Science, University of Southampton, where he is currently a Professor of intelligent systems and signal processing. He is a Distinguished Adjunct Professor with King Abdulaziz University, Jeddah, Saudi Arabia. He has published over 480 research papers. His recent research interests include adaptive signal processing, wireless communications, modeling and identification of nonlinear systems, neural network and machine learning, intelligent control system design, evolutionary computation methods, and optimization.

Dr. Chen is a Chartered Engineer and a Fellow of the Institution of Engineering and Technology. He was an Institute for Scientific Information highly cited researcher in the engineering category in March 2004.



Lajos Hanzo Lajos Hanzo (M'91–SM'92–F'04) received the M.S. degree (with first-class honors) in electronics and the Ph.D. degree from the Technical University of Budapest, Budapest, Hungary, in 1976 and 1983, respectively, the D.Sc. degree from the University of Southampton, Southampton, U.K., in 2004, and the "Doctor Honoris Causa" degree from the Technical University of Budapest in 2009.

During his 35-year career in telecommunications, he has held various research and academic posts in Hungary, Germany, and the U.K. Since 1986, he has

been with the School of Electronics and Computer Science, University of Southampton, Southampton, U.K., where he holds the Chair for Telecommunications. Since 2009, he has been a Chaired Professor with Tsinghua University, Beijing China. He is currently directing a 100-strong academic research team, working on a range of research projects in the field of wireless multimedia communications sponsored by industry; the Engineering and Physical Sciences Research Council, U.K.; the European IST Programme; and the Mobile Virtual Centre of Excellence, U.K. He is an enthusiastic supporter of industrial and academic liaison and offers a range of industrial courses. He has successfully supervised 80 Ph.D. students, coauthored 20 John Wiley/IEEE Press books on mobile radio communications totaling in excess of 10 000 pages, published more than 1250 research entries on IEEE Xplore, and presented keynote lectures. (For further information on research in progress and associated publications, please refer to <http://www-mobile.ecs.soton.ac.uk>.)

Dr. Hanzo is Fellow of the Royal Academy of Engineering, U.K., a Fellow of the Institution of Electrical Engineers, and a Governor of the IEEE Vehicular Technology Society. He has been a Technical Program Committee Chair and a General Chair for IEEE conferences. During 2008–2012, he was the Editor-in-Chief of the IEEE Press. He has received a number of distinctions.

AUTHOR QUERIES

AUTHOR PLEASE ANSWER ALL QUERIES

AQ1 = Note that “in the performance analysis section” was changed to “in Section III-D.4.”

AQ2 = Note that the section heading “The case of $(64 = 16 \times 4)$ -APSK” was changed to “ $(64 = 16 \times 4)$ -APSK” here and in another similar instance.

END OF ALL QUERIES

IEEE
Proof

A Universal Low-Complexity Symbol-to-Bit Soft Demapper

Qi Wang, Qiuliang Xie, Zhaocheng Wang, *Senior Member, IEEE*, Sheng Chen, *Fellow, IEEE*, and Lajos Hanzo, *Fellow, IEEE*

Abstract—High-order constellations are commonly used for achieving high bandwidth efficiency in most communication systems. However, the complexity of the multiplication operations associated with the standard max-sum approximation of the maximum *a posteriori* probability in the log-domain (Max-Log-MAP) symbol-to-bit demapper is very high. In this contribution, we conceive a low-complexity universal soft demapper, which reduces the demapper's complexity considerably for the binary-reflected Gray-labeled pulse amplitude modulation (PAM), phase shift keying (PSK), quadrature amplitude modulation (QAM), and amplitude phase-shift keying (APSK) relying on product constellation labeling (product-APSK). Our theoretical analysis demonstrates that the proposed demapper has exactly the same performance as the Max-Log-MAP demapper for the Gray-labeled PAM, PSK, and QAM. Our theoretical analysis and simulation results also demonstrate that for the Gray-labeled product-APSK, the performance degradation of the proposed simplified soft demapper is negligible for both 64-ary and 256-ary constellations compared with the Max-Log-MAP demapper.

Index Terms—Amplitude phase-shift keying (APSK), Max-Log-MAP, phase-shift keying (PSK), pulse amplitude modulation (PAM), quadrature amplitude modulation (QAM), soft demapper.

I. INTRODUCTION

HIGH-ORDER constellations are preferred in many transmission systems, as they are capable of achieving high bandwidth efficiency. For example, 256-ary quadrature amplitude modulation (256QAM) and 4096QAM are employed by the second-generation digital terrestrial television broadcasting standard (DVB-T2) [1] and the second-generation digital cable television broadcasting standard (DVB-C2) [2], respectively.

Manuscript received March 28, 2013; revised June 14, 2013; accepted June 30, 2013. This work was supported in part by the National Natural Science Foundation of China under Grant 61271266, by the National Key Basic Research Program of China under Grant 2013CB329203, and by the National High Technology Research and Development Program of China under Grant 2012AA011704. The review of this paper was coordinated by Prof. W. A. Hamouda.

Q. Wang and Z. Wang are with the Tsinghua National Laboratory for Information Science and Technology, Department of Electronic Engineering, Tsinghua University, Beijing 100084, China (e-mail: qiwang11@mails.tsinghua.edu.cn; zewang@mail.tsinghua.edu.cn).

Q. Xie is with the Department of Radiation Oncology, University of California, Los Angeles, CA 90024 USA (e-mail: xieqiuliang@gmail.com).

S. Chen is with Electronics and Computer Science, University of Southampton, Southampton SO17 1BJ, U.K., and also with King Abdulaziz University, Jeddah 21589, Saudi Arabia (e-mail: sqc@ecs.soton.ac.uk).

L. Hanzo is with Electronics and Computer Science, University of Southampton, Southampton SO17 1BJ, U.K. (e-mail: lh@ecs.soton.ac.uk).

Color versions of one or more of the figures in this paper are available online at <http://ieeexplore.ieee.org>.

Digital Object Identifier 10.1109/TVT.2013.2272640

Furthermore, 128QAM is recommended by the long-term evolution advanced (LTE-Advanced) standards [3], which supports reception even for high-velocity vehicular communications. However, for these high-order modulation schemes, a high-complexity symbol-to-bit demapper is required when using the conventional maximum *a posteriori* probability based in the log-domain (Log-MAP) demapping algorithm [4]. Albeit the max-sum-approximation-based version of the Log-MAP (Max-Log-MAP) demapper [5] eliminates the high-complexity exponential and logarithmic operations in the Log-MAP algorithm, the number of multiplications remains high, and the complexity of the Max-Log-MAP algorithm is on the order of $O(2^m)$, where 2^m denotes the constellation size with m representing the number of bits per symbol.

Numerous simplified demapper algorithms have been proposed for specific constellations. In [6], a bit-metric-generation approach is proposed for phase-shift keying (PSK) using Gray labeling, which recursively generates bit metrics based on a simplified function. This recursive demapper achieves the same performance as the Max-Log-MAP demapper, while reducing the number of multiplications by 59% for 32PSK. By decomposing the 2^m -ary QAM constellation into two independent ($2^{m/2}$ -ary pulse amplitude modulation (PAM) constellations, the complexity of the associated Max-Log-MAP demapper is reduced from $O(2^m)$ to $O(2^{m/2})$ [7], [8]. The complexity of the QAM demapper can be further reduced to the order of $O(m)$ by invoking a piecewise linear approximation, but this inevitably imposes performance degradation [9]. A similar soft demapper is proposed for amplitude PSK (APSK) in [10], where the constellation is partitioned with the aid of simplified hard-decision threshold (HDT)-based boundaries, and soft information is calculated as the distances between the received signal and the HDT lines. This approximate demapper reduces the number of multiplications to 4 and 11 for 16APSK and 32APSK, respectively. A simplified demapper is also proposed for multilevel coding followed by multistage decoding, which focuses on the APSK signal [11], and the complexity of this APSK demapper is reduced to a constant (neglecting comparison operations) at the cost of exponentially increasing the memory required and necessitating an additional division [11]. In [12], the complexity of the demapper is reduced by reusing the multipliers, and only 16 multipliers are used for all the four modulation modes (QPSK, 8PSK, 16APSK, and 32APSK) in the second-generation digital video broadcasting over satellite (DVB-S2) system. For the constellation rotation and cyclic Q delay modulation of DVB-T2, several simplified demappers are proposed for reducing

complexity by decreasing the number of the constellation points required for calculating the minimum squared distances [13]–[15]. For APSK using product constellation labeling (product-APSK), it is shown [16] that a $(2^{m_1} \times 2^{m_2} = 2^m)$ -ary APSK constellation can be regarded as the product of 2^{m_1} -ary PSK and pseudo 2^{m_2} -ary PAM, and a simplified demapper is proposed in [17], which reduces the complexity of the demapper from $O(2^m)$ to $O(2^{m_1}) + O(2^{m_2})$.

All the previously mentioned Gray labeling functions designed for the various constellations are the classic binary-reflected Gray labeling schemes proposed by Gray in 1953 as a means of reducing the number of bit errors, where two adjacent constellation points differ in only one bit [18]. In [19], Agrell *et al.* showed that the binary-reflected Gray labeling is the optimal labeling for PAM, PSK, and QAM, which achieves the lowest possible bit error probability among all possible labeling functions for the additive white Gaussian noise (AWGN) channel.

Against this background, in this contribution, a universal low-complexity soft demapper is proposed for various binary-reflected Gray-labeled constellations. By exploiting the symmetry of Gray-labeled constellations, we show that the complexity of a 2^m -ary demapper can be reduced from $O(2^m)$ to $O(m)$. Moreover, our proposed low-complexity soft demapper attains the same performance as the Max-Log-MAP demapper for PAM, PSK, and QAM, whereas the performance degradation of our low-complexity soft demapper is negligible for product-APSK, in comparison with the Max-Log-MAP solution.

The rest of this paper is organized as follows. In Section II, the standard Max-Log-MAP demapper is highlighted. In Section III, our simplified soft demapper is proposed, and its performance and complexity are analyzed in detail. In Section IV, the performance of both the proposed low-complexity demapper and the conventional Max-Log-MAP demapper is quantified for Gray-labeled QAM and product-APSK for transmission over both AWGN and Rayleigh fading channels. Our conclusions are drawn in Section V.

The following notations are employed throughout this contribution. Uppercase calligraphic letters denote sets, e.g., \mathcal{X} . Boldface lowercase letters represent vectors, e.g., \mathbf{b} , whose i th element is written as b_i . Uppercase letters denote random variables (RVs), e.g., X , whereas the corresponding lowercase letters represent their realizations, e.g., x . $P(x)$ is used for the probability mass function (pmf) of a discrete RV X , and $p(x)$ denotes the probability density function (pdf) of a continuous RV X . $P(y|x)$ represents the conditional pmf of $Y = y$ given $X = x$, whereas $p(y|x)$ represents the conditional pdf of $Y = y$ given $X = x$. The magnitude operator is denoted by $|\cdot|$.

II. SYSTEM MODEL WITH MAX-LOG-MAXIMUM

A POSTERIORI DEMAPPER

At the transmitter of a coded system, the coded bits are grouped into bit vectors, each with the length of m and denoted by $\mathbf{b} = (b_0 \ b_1 \ \dots \ b_{m-1})$. Bit vector \mathbf{b} is then mapped onto constellation point $x \in \mathcal{X}$ for transmission, where $\mathcal{X} = \{x_k, 0 \leq k < 2^m\}$ denotes the signal set of size 2^m .

At the receiver, the soft information for each coded bit is calculated based on received signal y , which is then passed to the decoder. For the Log-MAP demapper, the soft information on the i th bit is expressed in the form of the log-likelihood ratio (LLR) L_i according to [17]

$$\begin{aligned} L_i &= \log \frac{P(b_i = 0|y)}{P(b_i = 1|y)} = \log \frac{\sum_{x \in \mathcal{X}_i^{(0)}} P(x|y)}{\sum_{x \in \mathcal{X}_i^{(1)}} P(x|y)} \\ &= \log \frac{\sum_{x \in \mathcal{X}_i^{(0)}} p(y|x)}{\sum_{x \in \mathcal{X}_i^{(1)}} p(y|x)} \end{aligned} \quad (1)$$

for $0 \leq i < m$, where $\mathcal{X}_i^{(b)}$ denotes the signal subset of \mathcal{X} with the i th bit being $b \in \{0, 1\}$. The last equality in (1) follows from Bayes' rule and the assumption that signals $x_k, 0 \leq k < 2^m$ are equiprobable.

A flat-fading channel is modeled as $y = hx + n$, where h denotes the complex-valued channel state information (CSI), and n stands for the complex-valued AWGN with zero mean and variance $N_0/2$ per dimension. When the perfect CSI h is available at the receiver, the conditional pdf $p(y|x)$ in (1) can be written as $p(y|x) = (1/\pi N_0) \exp(-|y - hx|^2/N_0)$. Observe that given the availability of perfect CSI, the received signal can be phase equalized, after which only the amplitude of CSI h is required. Thus, we simply assume that h is nonnegative real valued. By using the well-known max-sum approximation of $\sum_j z_j \approx \max_j z_j$ for nonnegative z_j , where the summation is dominated by the largest term, the conventional Max-Log-MAP demapper is readily formulated as

$$\begin{aligned} L_i &\approx \log \frac{\max_{x \in \mathcal{X}_i^{(0)}} p(y|x)}{\max_{x \in \mathcal{X}_i^{(1)}} p(y|x)} \\ &= -\frac{1}{N_0} \left(\min_{x \in \mathcal{X}_i^{(0)}} |y - hx|^2 - \min_{x \in \mathcal{X}_i^{(1)}} |y - hx|^2 \right). \end{aligned} \quad (2)$$

The Max-Log-MAP of (2) is a fairly accurate approximation of the Log-MAP of (1) in the high signal-to-noise ratio (SNR) region, and it avoids the complex exponential and logarithmic operations. For each received signal, the Max-Log-MAP demapper calculates all the 2^m squared Euclidean distances, i.e., $|y - hx|^2$ for every $x \in \mathcal{X}$, to find the two minimum terms described in (2). Therefore, its complexity quantified in terms of multiplications is on the order of $O(2^m)$.

III. PROPOSED SIMPLIFIED SOFT DEMAPPER

After carefully examining (2), it is interesting to note that item $\min_{x \in \mathcal{X}} |y - hx|^2$, i.e., the squared Euclidean distance from received signal y to the nearest constellation point x^* , always appears in (2), and it is equal to either $\min_{x \in \mathcal{X}_i^{(0)}} |y - hx|^2$ or $\min_{x \in \mathcal{X}_i^{(1)}} |y - hx|^2$, depending on the i th bit of x^* being 0 or 1. In other words, $|y - hx^*|^2$ is always one of the two terms in (2). By denoting the bit vector that maps to signal x^* as $\mathbf{b}^* = (b_0^* \ b_1^* \ \dots \ b_{m-1}^*)$, the other item in (2) represents the squared Euclidean distance from y to the nearest constellation

179 point in subset $\mathcal{X}_i^{(\bar{b}_i^*)}$, which is denoted by $x_{i,\bar{b}_i^*}^*$, where we have

180 $\bar{b} = 1 - b$.

181 For Gray-labeled constellations, we will show that x^* and
182 $x_{i,\bar{b}_i^*}^*$, $0 \leq i < m$, can be determined by using simple compar-
183 ison and addition operations. Afterward, we only have to cal-
184 culate the $m + 1$ squared Euclidean distances, i.e., $|y - hx^*|^2$
185 and $|y - hx_{i,\bar{b}_i^*}^*|^2$ for $0 \leq i < m$. Therefore, the complexity of
186 our proposed demapper is on the order of $O(m)$.

187 Accordingly, we divide the demapping procedure into three
188 steps: 1) finding x^* and \mathbf{b}^* ; 2) determining $x_{i,\bar{b}_i^*}^*$; and
189 3) calculating L_i according to (2). For binary-reflected Gray-
190 labeled constellations, we have the following lemma from [20],
191 describing how to obtain \mathbf{b}^* .

192 **Lemma 1:** For binary-reflected Gray labeling $\mathbf{b} \rightarrow x_k$, by
193 denoting $\mathbf{c}^k = (c_0^k \ c_1^k \ \dots \ c_{m-1}^k)$ as the binary representation
194 of index k with the least significant bit (LSB) as the rightmost
195 bit, \mathbf{b} can be calculated as

$$\mathbf{b} = (c_0^k \ c_1^k \ \dots \ c_{m-1}^k) \oplus (0 \ c_0^k \ \dots \ c_{m-2}^k) \quad (3)$$

196 where \oplus represents the bitwise XOR operation.

197 The expressions generated for determining x^* and $x_{i,\bar{b}_i^*}^*$ are
198 slightly different for various constellations. In the following, the
199 simplified soft demappers designed for the Gray-labeled PAM,
200 QAM, PSK, and product-APSK are presented in detail.

201 A. PAM Demapper

202 Without loss of generality, we assume that all the signals as-
203 sociated with PAM are real valued. For the 2^m -ary Gray-labeled
204 PAM, we denote the constellation points as $x_0, x_1, \dots, x_{2^m-1}$
205 with the k th constellation point x_k given by $x_k = \delta(-(2^m -$
206 $1) + 2k)/2$, where δ denotes the distance between each pair
207 of adjacent constellation points. The detailed PAM demapping
208 procedure is given as follows.

- 209 1) *Find x^* and \mathbf{b}^* .* For 2^m -PAM, signal space can be di-
210 vided into 2^m intervals separated by amplitude thresholds
211 $-(2^{m-1} - 1)\delta, -(2^{m-1} - 2)\delta, \dots, (2^{m-1} - 1)\delta$. Mul-
212 tiplying h with the thresholds can be implemented by
213 SHIFT-ADD operations, since the thresholds are constants.
214 Additionally, we can use the binary-search algorithm to
215 find the specific interval in which y is located. Therefore,
216 only m comparison operations are required for obtaining
217 $x^* = x_{k^*}$. The corresponding bit vector \mathbf{b}^* can then be
218 calculated according to Lemma 1. An example for the
219 Gray-labeled 8PAM (Gray-8PAM) constellation is shown
220 in Fig. 1, where we have $k^* = 2$ and $\mathbf{b}^* = (0 \ 1 \ 1)$.
- 221 2) *Determine $x_{i,\bar{b}_i^*}^*$.* Considering the symmetric structure
222 of Gray-labeled PAM constellations, we have the fol-
223 lowing lemma for computing $x_{i,\bar{b}_i^*}^*$, which only requires
224 the binary representation of k^* and addition operations,
225 instead of the need to calculate all the squared Euclidean
226 distances from y to the constellation points in subset
227 $\mathcal{X}_i^{(\bar{b}_i^*)}$ and compare all the resultant 2^{m-1} metrics.

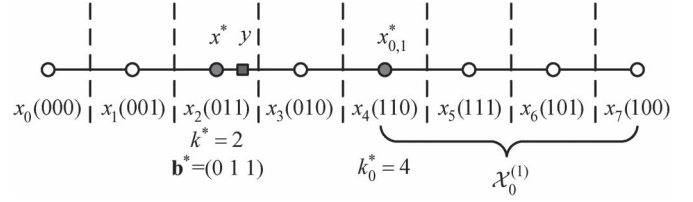


Fig. 1. Gray-8PAM constellation and illustration of demapping for the 0th bit over the AWGN channel.

Lemma 2: For the binary-reflected Gray PAM $\mathbf{b}^* \rightarrow x_{k^*}$, 228
where x_{k^*} is the nearest constellation point to received signal 229
 y , let $\mathbf{c}^{k^*} = (c_0^{k^*} \ c_1^{k^*} \ \dots \ c_{m-1}^{k^*})$ be the binary representation 230
of k^* with the LSB as the rightmost bit. Then, the nearest 231
constellation point to y in subset $\mathcal{X}_i^{(\bar{b}_i^*)}$, namely, $x_{i,\bar{b}_i^*}^*$, can be 232
determined according to 233

$$x_{i,\bar{b}_i^*}^* = x_{k_i^*} \quad (4)$$

where

$$k_i^* = 2^{m-i-1} - c_i^{k^*} + \sum_{j=0}^{i-1} c_j^{k^*} 2^{m-j-1}. \quad (5)$$

Proof: See Appendix A. ■ 235

- 3) *Calculate L_i according to (2).* After obtaining x^* , \mathbf{b}^* , and 236
 $x_{i,\bar{b}_i^*}^*$, we can rewrite L_i as 237

$$L_i = -\frac{1}{N_0} (1 - 2b_i^*) \left(|y - hx^*|^2 - |y - hx_{i,\bar{b}_i^*}^*|^2 \right). \quad (6)$$

It is clear that (6) is equivalent to (2) for the Gray-labeled 238
PAM. Hence, the performance of the proposed simplified soft 239
demapper is exactly the same as that of the standard Max-Log- 240
MAP demapper, while its complexity is reduced from $O(2^m)$ 241
to $O(m)$. 242

243 B. QAM Demapper

The 2^m -ary square Gray-labeled QAM can be decomposed 244
into two independent (in-phase and quadrature phase) $2^{m/2}$ -ary 245
Gray-labeled PAMs, and we can apply our proposed simplified 246
PAM demapper to each of these two Gray-labeled PAMs. Thus, 247
the complexity of our simplified Gray-labeled QAM demapper 248
is reduced from $O(2^m)$ to $O(m)$ without suffering any per- 249
formance loss, in comparison to the standard Max-Log-MAP 250
demapper. 251

252 C. PSK Demapper

By applying the same idea to PSK demapping, we can 253
also reduce the complexity from $O(2^m)$ to $O(m)$ without any 254
performance loss, compared with the Max-Log-MAP solution. 255
For 2^m -ary Gray-labeled PSK, the signal set can be written 256
in the polar coordinate format as $\mathcal{X} = \{x_k = \sqrt{E_s} \exp(j(2k +$ 257
 $1)\pi/2^m)\}$, $0 \leq k < 2^m$, where E_s denotes the energy of the 258
transmitted signals, and $j = \sqrt{-1}$. An example of the Gray- 259
8PSK constellation is shown in Fig. 2. 260

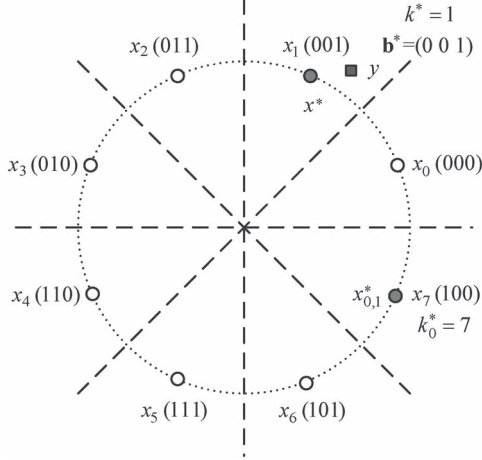


Fig. 2. Gray-8PSK constellation and illustration of demapping for the zeroth bit over the AWGN channel.

Let us express the phase-equalized received signal y in the polar coordinate format as $y = \rho_y \exp(j\varphi_y)$, where ρ_y and φ_y denote the amplitude and phase of y , respectively, and $0 \leq \varphi_y < 2\pi$. Then, the squared Euclidean distance $|y - hx|^2$ can be written as

$$\begin{aligned} |y - hx|^2 &= \left| \rho_y \exp(j\varphi_y) - h\sqrt{E_s} \exp(j\varphi_x) \right|^2 \\ &= \rho_y^2 + h^2 E_s - 2\rho_y h \sqrt{E_s} \cos(\varphi_x - \varphi_y) \\ &= \rho_y^2 + h^2 E_s - 2\rho_y h \sqrt{E_s} \cos(\phi(x, y)) \end{aligned} \quad (7)$$

where φ_x is the phase of x , and $\phi(x, y)$ is defined as

$$\phi(x, y) = \begin{cases} |\varphi_x - \varphi_y|, & 0 \leq |\varphi_x - \varphi_y| \leq \pi \\ 2\pi - |\varphi_x - \varphi_y|, & \pi < |\varphi_x - \varphi_y| < 2\pi \end{cases} \quad (8)$$

It is obvious that $\phi(x, y) \in [0, \pi]$ and is commutative, i.e., $\phi(x, y) = \phi(y, x)$. The mapping defined in (8) also satisfies the triangle inequality, that is, $\forall x, y, z \in \mathbb{C}$, we have

$$\phi(x, z) \leq \phi(x, y) + \phi(y, z) \quad (9)$$

where \mathbb{C} denotes the complex-valued space. The proof is given in Appendix B. Therefore, $\phi(x, y)$ defines a distance over \mathbb{C} , which is referred to as the *phase distance* of x and y in this paper.

Furthermore, multiplying $x \in \mathbb{C}$ with a positive value does not change the phase of x , i.e., $\varphi_{hx} = \varphi_x, \forall h > 0$. Hence, we have $\phi(hx, y) = \phi(x, y), \forall h > 0$. Since the cosine function is a decreasing function in $[0, \pi]$, minimizing the squared Euclidean distance $|y - hx|^2$ of (7) is equivalent to minimizing phase distance $\phi(x, y)$. Therefore, we can simply use the phase of the signal in the search process of the PSK demapper, and the resultant PSK demapping procedure is detailed as follows.

1) *Find x^* and \mathbf{b}^* .* The signal space of the 2^m -ary Gray-labeled PSK can be divided into 2^m phase intervals separated by phase thresholds $0, \pi/2^{m-1}, \dots, (2^m - 1)\pi/2^{m-1}$, as shown in Fig. 2. Signal x^* can be obtained by comparing φ_y with the phase thresholds, which only needs m comparisons using the binary-search algorithm.

Similar to the PAM demapper, after finding $x^* = x_{k^*}$, the corresponding bit vector \mathbf{b}^* is calculated according to Lemma 1. For the case shown in Fig. 2, we have $k^* = 1$ and $\mathbf{b}^* = (0 0 1)$.

2) *Determine $x_{i, \mathbf{b}_i^*}^*$.* Unlike the PAM constellation, the PSK constellation is circularly symmetric, and the phase distance function we used for comparisons is defined in a piecewise fashion. Therefore, calculating $x_{i, \mathbf{b}_i^*}^*$ for the PSK demapper is slightly different from that of the PAM demapper. We have the following lemma for computing $x_{i, \mathbf{b}_i^*}^*$ of Gray-labeled PSK.

Lemma 3: For the binary-reflected Gray PSK $\mathbf{b}^* \rightarrow x_{k^*}$, where x_{k^*} is the constellation point nearest to received signal y , let $\mathbf{c}^{k^*} = (c_0^{k^*} c_1^{k^*} \dots c_{m-1}^{k^*})$ be the binary representation of k^* with the LSB as the rightmost bit. Then, the point nearest to y in subset $\mathcal{X}_i^{(\mathbf{b}_i^*)}$, namely, $x_{i, \mathbf{b}_i^*}^*$, can be determined according to

$$x_{i, \mathbf{b}_i^*}^* = x_{k_i^*} \quad (10)$$

where

$$k_i^* = \begin{cases} c_0^{k^*} 2^{m-1} + c_1^{k^*} (2^{m-1} - 1), & i = 0 \\ 2^{m-i-1} - c_i^{k^*} + \sum_{j=0}^{i-1} c_j^{k^*} 2^{m-j-1}, & i > 0 \end{cases} \quad (11)$$

Proof: See Appendix C. ■

3) *Calculate L_i according to (2).* After obtaining x^*, \mathbf{b}^* , and $x_{i, \mathbf{b}_i^*}^*$, the soft information on the i th bit, i.e., L_i , is calculated according to (6), which is the same result as that in (2) for the Max-Log-MAP demapper, as is the case for the PAM demapper. Clearly, the performance of this simplified soft demapper is identical to that of the Max-Log-MAP demapper, while only imposing a complexity on the order of $O(m)$.

D. Gray-APSK Demapper

1) *Review of Gray-APSK:* A generic M -ary APSK constellation is composed of R concentric rings, each having uniformly spaced PSK points. More specifically, the M -APSK constellation set is given by $\mathcal{X} = \{r_l \exp(j(2\pi i/n_l + \theta_l)), 0 \leq i < n_l, 0 \leq l < R\}$, in which n_l, r_l , and θ_l denote the number of PSK points, the radius, and the phase shift of the l th ring, respectively, while we have $\sum_{l=0}^{R-1} n_l = M$ [21].

In [16], a special APSK constellation was proposed, which consists of $R = 2^{m_2}$ rings and $n_l = 2^{m_1}$ PSK points on each ring for the $(M = 2^m)$ -ary APSK, where we have $m_1 + m_2 = m$. This kind of APSK is known as the product-APSK and is denoted by $(M = 2^{m_1} \times 2^{m_2})$ -APSK. The l th radius of the product-APSK constellation, where $0 \leq l < R$, is determined by

$$r_l = \sqrt{-\ln(1 - (l + 1/2)2^{-m_2})}. \quad (12)$$

The $(2^m = 2^{m_1} \times 2^{m_2})$ -APSK can be regarded as the product of 2^{m_1} -ary PSK and 2^{m_2} -ary pseudo PAM, where the

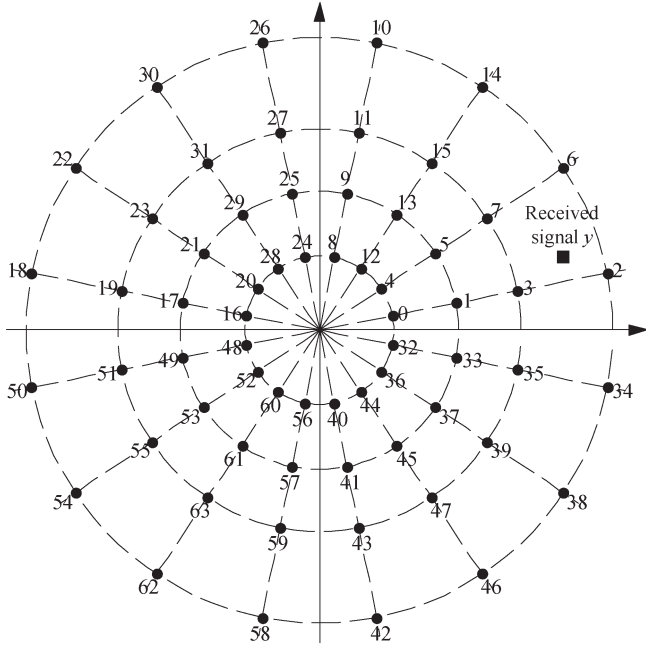


Fig. 3. Gray-labeled $(64 = 16 \times 4)$ -APSK constellation, where the labels are in the decimal form with the binary representation having the LSB as the rightmost bit.

332 pseudo PAM and PSK sets are given, respectively, by $\mathcal{A} =$
 333 $\{r_l, 0 \leq l < 2^{m_2}\}$ and $\mathcal{P} = \{p_k = \exp(j\varphi_k) \text{ with } \varphi_k = (2k +$
 334 $1)\pi/2^{m_1}, 0 \leq k < 2^{m_1}\}$ [17]. We divide the m -bit vector
 335 \mathbf{b} into two subvectors \mathbf{b}^P and \mathbf{b}^A of lengths m_1 and m_2 ,
 336 respectively. Specifically, \mathbf{b}^P consists of the leftmost m_1 bits
 337 of \mathbf{b} , whereas \mathbf{b}^A contains the rest rightmost m_2 bits of \mathbf{b} .
 338 Without loss of generality, \mathbf{b}^P is mapped to the equivalent 2^{m_1} -
 339 PSK point, and \mathbf{b}^A is mapped to the equivalent pseudo 2^{m_2} -
 340 PAM point. Gray labeling can be used for mapping the bits to
 341 the equivalent constellation signals. This Gray-labeled APSK
 342 (Gray-APSK) is a special product-APSK [16], [17]. The Gray-
 343 labeled $(64 = 16 \times 4)$ -APSK is shown in Fig. 3.

344 2) *Proposed Demapping Algorithm for Gray-APSK*: Like
 345 the other constellations previously discussed, the standard Max-
 346 Log-MAP demapping designed for Gray-APSK also uses (2).
 347 By writing transmitted signal x and received signal y in the
 348 polar-coordinate format, the squared Euclidean distance $|y -$
 349 $hx|^2$ for Gray-APSK can be readily expressed as

$$\begin{aligned} |y - hx|^2 &= \rho_y^2 + h^2 \rho_x^2 - 2h\rho_x \rho_y \cos(\phi(x, y)) \\ &= (\rho_y \cos(\phi(x, y)) - h\rho_x)^2 + \rho_y^2 \sin^2(\phi(x, y)) \end{aligned} \quad (13)$$

350 where ρ_x and ρ_y represent the amplitudes of x and y , respec-
 351 tively, and $\phi(x, y)$ is the phase distance between x and y , as
 352 defined in (8).

353 Due to the circular symmetry of the Gray-APSK constella-
 354 tion, it is clear that the nearest constellation point x^* from y
 355 has the smallest phase distance, i.e., $\phi(x^*, y)$ is the smallest
 356 one in set $\{\phi(x, y), \varphi_x \in \mathcal{P}\}$, and it is no larger than $\pi/2^{m_1}$,
 357 as exemplified in Fig. 3. Furthermore, according to (13), the
 358 amplitude of x^* , which is denoted by ρ_{x^*} , satisfies

$$\rho_{x^*} = \arg \min_{\rho_x \in \mathcal{A}} |\rho_y \cos(\phi(x^*, y)) - h\rho_x|. \quad (14)$$

After determining the phase and the amplitude of x^* , it is easy 359
 to find the corresponding bit label \mathbf{b}^* . As for finding $x_{i, \mathbf{b}_i^*}^*$, this 360
 depends on whether the i th bit is related to the phase or the 361
 amplitude. 362

For the bits related to the phase of the Gray-APSK signal, 363
 i.e., for $0 \leq i < m_1$, the phase of $x_{i, \mathbf{b}_i^*}^*$, which is denoted by 364
 $\varphi_{x_{i, \mathbf{b}_i^*}^*}$, can be readily determined based on Lemma 3 owing to 365
 the uniform distribution of the phases, whereas the amplitude 366
 of $x_{i, \mathbf{b}_i^*}^*$, which is denoted by $\rho_{x_{i, \mathbf{b}_i^*}^*}$, obeys 367

$$\rho_{x_{i, \mathbf{b}_i^*}^*} = \arg \min_{\rho_x \in \mathcal{A}} \left| \rho_y \cos\left(\phi\left(x_{i, \mathbf{b}_i^*}^*, y\right)\right) - h\rho_x \right|. \quad (15)$$

For the bits mapped to the amplitude of the Gray-APSK 368
 signal, i.e., for $m_1 \leq i < m$, it is clear that the phase of $x_{i, \mathbf{b}_i^*}^*$ 369
 is exactly the same as that of x^* , and we may approximately 370
 obtain the amplitude of $x_{i, \mathbf{b}_i^*}^*$ via Lemma 2. However, due to the 371
 nonuniformly spaced amplitudes of \mathcal{A} , such an approximation 372
 may cause some errors, albeit the performance loss is fortu- 373
 nately negligible, as will be detailed later in Section III-D4. 374

Upon obtaining x^* , \mathbf{b}^* , and $x_{i, \mathbf{b}_i^*}^*$, we can readily determine 375
 the demapping output of the i th bit based on (6). This simplified 376
 Gray-APSK demapping procedure is summarized as follows. 377

- 1) *Find x^* and \mathbf{b}^** . The phase of x^* is determined by 378
 minimizing the phase difference from y to x with phase 379
 $\varphi_x \in \mathcal{P}$, and its amplitude is determined according to 380
 (14). Having obtained $\varphi_{x^*} = \varphi_{k^*P^*}$ and $\rho_{x^*} = r_{k^*A^*}$, sub- 381
 bit vectors \mathbf{b}^{P^*} and \mathbf{b}^{A^*} are calculated according to 382
 Lemma 1, yielding $\mathbf{b}^* = (\mathbf{b}^{P^*} \mathbf{b}^{A^*})$. 383
- 2) *Determine $x_{i, \mathbf{b}_i^*}^*$* . For the leftmost m_1 bits that are related 384
 to the phases of the Gray-APSK signals, we can obtain 385
 the phase of $x_{i, \mathbf{b}_i^*}^*$ according to Lemma 3 and its amplitude 386
 according to (15). For the rightmost m_2 bits, i.e., $m_1 \leq$ 387
 $i < m$, the phase of $x_{i, \mathbf{b}_i^*}^*$ is exactly the same as φ_{x^*} , and 388
 its amplitude is approximately determined according to 389
 Lemma 2. 390
- 3) *Calculate L_i according to (2)*. After obtaining x^* , \mathbf{b}^* , and 391
 $x_{i, \mathbf{b}_i^*}^*$, the soft information on the i th bit, i.e., L_i , is given 392
 by (6), as for the other demappers. 393

3) *Complexity Analysis*: Step 1) determines x^* and \mathbf{b}^* . The 394
 phase of x^* can be readily obtained by simple comparison 395
 operations, and its amplitude is determined according to (14), 396
 which requires one multiplication for $\rho_y \cos(\phi(x^*, y))$ and 397
 m_2 comparison operations. Having determined x^* , calculating 398
 \mathbf{b}^* only requires some low-complexity XOR operations. The 399
 complexity of step 2) is mainly associated with determining the 400
 amplitude of $x_{i, \mathbf{b}_i^*}^*$ according to (15), for $0 \leq i < m_1$, which 401
 requires one multiplication operation for $\rho_y \cos(\phi(x_{i, \mathbf{b}_i^*}^*, y))$ 402
 and m_2 comparison operations. It is therefore clear that the 403
 complexity of the proposed simplified Gray-APSK demapper 404
 is $O(2 \times m_1 + m_2) \approx O(m)$, which is dramatically lower than 405
 the complexity of $O(2^m)$ required by the standard Max-Log- 406
 MAP solution. 407

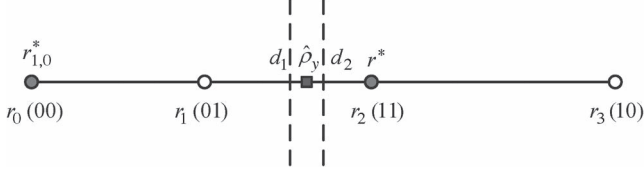


Fig. 4. Pseudo4PAM decomposed from the $(64 = 16 \times 4)$ -APSK constellation.

An alternative complexity analysis, which is “easier” to follow is outlined below. The demapper proposed for $(2^m = 2^{m_1} \times 2^{m_2})$ -APSK is equivalent to the demapper conceived for 2^{m_1} -ary PSK implemented with the aid of the simplified PSK demapping procedure in Section III-C at the complexity of $O(m_1)$ and the demapper for the 2^{m_2} -ary pseudo PAM implemented with the aid of the simplified PAM demapping procedure in Section III-A at the complexity of $O(m_2)$. Therefore, the complexity of the proposed simplified Gray-APSK demapper is approximately $O(m_1) + O(m_2) \approx O(m)$. It is worth emphasizing again that the complexity of our proposed simplified Gray-APSK demapper is also much lower than that of the simplified soft demapper for product-APSK given in [17], which is on the order of $O(2^{m_1}) + O(2^{m_2})$.

4) *Performance Analysis*: Owing to the fact that the phase of the APSK constellation is uniformly spaced, Lemma 3 always holds when demapping the leftmost m_1 bits, and the results of the proposed demapper are exactly the same as those of the Max-Log-MAP demapper. However, unlike in the conventional PAM, the distances between pairs of adjacent points in the corresponding pseudo PAM part of the Gray-APSK constellation are not constant, which means that Lemma 2 does not always hold. Therefore, when demapping the rightmost m_2 bits with the aid of Lemma 2, the resultant x_{i, \bar{b}_i}^* may

not always be the point nearest to y in subset $\mathcal{X}_i^{(\bar{b}_i^*)}$, which may slightly increase the absolute value of the LLR in (2) and, consequently, results in some performance degradation. Fortunately, this degradation is negligible. In the following, we present the detailed analysis of this performance loss with the aid of Gray-labeled 64-APSK and 256-APSK.

a) $(64 = 16 \times 4)$ -APSK: As shown in Fig. 4, to demap the rightmost 2 bits related to the amplitudes in the $(64 = 16 \times 4)$ -APSK, we have the scalar projection of y in the direction of φ_{x^*} and the pseudo Gray 4PAM constellation set \mathcal{A} . We denote the projection as $\hat{\rho}_y = \rho_y \cos(\phi(x^*, y))$ and the thresholds as $d_1 = (r_1 + r_2)/2$ and $d_2 = (r_0 + r_3)/2$. If $\hat{\rho}_y$ is smaller than d_1 , we have $r^* = r_0$ or r_1 , and the zeroth bit of \mathbf{b}^{A^*} must be 0. The constellation subset with the zeroth bit being 1 is $\mathcal{A}_0^{(1)} = \{r_2, r_3\}$, and obviously, the nearest point to $\hat{\rho}_y$ in $\mathcal{A}_0^{(1)}$ is $r_{0,1}^* = r_2$, which is identical to the result given by Lemma 2. If $\hat{\rho}_y$ is larger than d_1 , we have $b_0^{A^*} = 1$ and $r_{0,0}^* = r_1$, which is also the same result given by Lemma 2. Therefore, the proposed demapper achieves the same result as the Max-Log-MAP demapper for the zeroth bit of the pseudo 4PAM, and no error is introduced.

However, for the first bit of the pseudo 4PAM, when $\hat{\rho}_y$ falls in the interval of (d_1, d_2) known as the *error interval*,¹

¹Here, we have $d_1 < d_2$ according to (12).

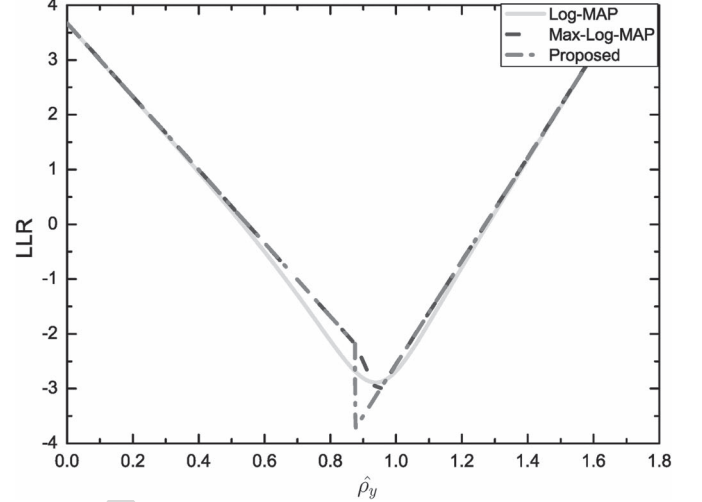


Fig. 5. LLR of the first bit of the pseudo 4PAM decomposed from $(64 = 16 \times 4)$ -APSK over the AWGN channel with $E_s/N_0 = 10$ dB.

the nearest constellation point to $\hat{\rho}_y$ in \mathcal{A} is $r^* = r_2$, and we have $\mathbf{b}^{A^*} = (1 \ 1)$ and $\mathcal{A}_1^{(0)} = \{r_0, r_3\}$. The point nearest to $\hat{\rho}_y$ in $\mathcal{A}_1^{(0)}$ is supposed to be $r_{1,0}^* = r_3$ according to Lemma 2, but in fact, $\hat{\rho}_y$ is closer to r_0 because of the asymmetry of the pseudo PAM. The proposed demapper uses a farther point that increases the absolute value of the LLR in (2). The increment of the absolute value of the LLR caused by the proposed demapper is bounded by

$$\begin{aligned} \Delta L &= (|\hat{\rho}_y - r_3|^2 - |\hat{\rho}_y - r_0|^2) / N_0 \\ &= (r_3 - r_0)(r_0 + r_3 - 2\hat{\rho}_y) / N_0 \\ &< (r_3 - r_0)(r_0 + r_3 - r_1 - r_2) / N_0. \end{aligned} \quad (16)$$

The exact and correct absolute LLR value is

$$\begin{aligned} |L_1| &= (|\hat{\rho}_y - r_0|^2 - |\hat{\rho}_y - r_2|^2) / N_0 \\ &= (r_2 - r_0)(2\hat{\rho}_y - r_0 - r_2) / N_0 \\ &> (r_2 - r_0)(r_1 - r_0) / N_0. \end{aligned} \quad (17)$$

Therefore, the ratio of ΔL over $|L_1|$ is bounded by

$$\frac{\Delta L}{|L_1|} < \frac{(r_3 - r_0)(r_3 + r_0 - r_1 - r_2)}{(r_2 - r_0)(r_1 - r_0)} \approx 0.708. \quad (18)$$

The LLRs of the first bit of the pseudo 4PAM calculated by the Log-MAP, Max-Log-MAP, and our proposed demapper are shown in Fig. 5. The LLR calculated by our proposed demapper is exactly the same as that of the Max-Log-MAP demapper when $\hat{\rho}_y$ is outside the interval (d_1, d_2) . When $d_1 < \hat{\rho}_y < d_2$, the absolute value of the LLR calculated by our proposed demapper is slightly larger than that of the Max-Log-MAP demapper. It is interesting to note that the absolute value of the LLR calculated by the Log-MAP demapper is also slightly larger than that of the Max-Log-MAP demapper in some regions, and it is worth remembering that the Max-Log-MAP solution itself is an approximation of the optimal Log-MAP solution.

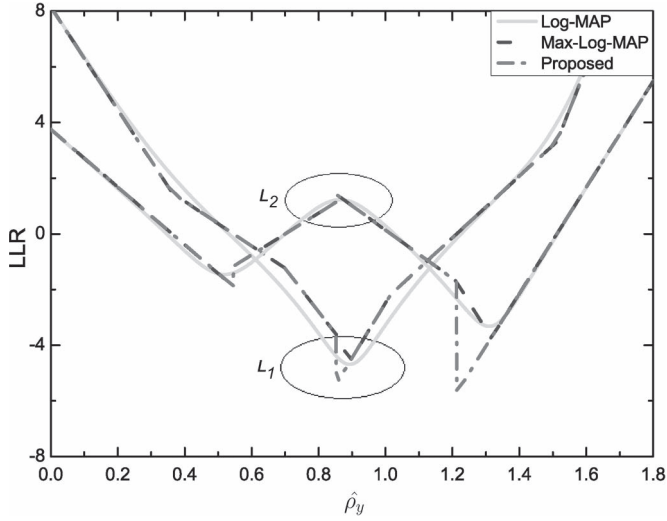


Fig. 6. LLRs of the first and second bits of the pseudo 8PAM decomposed from (256 = 32 × 8)-APSK over the AWGN channel with $E_s/N_0 = 14$ dB.

The ratio (18) associated with the error is an upper bound. Furthermore, this error only exists when $\hat{\rho}_y \in (d_1, d_2)$, which does not frequently happen, as will be detailed later. Before analyzing the probability of $\hat{\rho}_y$ falling into an error interval, we further examine the larger constellation of (256 = 32 × 8)-APSK.

b) (256 = 32 × 8)-APSK: Similar to (64 = 16 × 4)-APSK, for (256 = 32 × 8)-APSK, the error also occurs when demapping the rightmost 3 bits, since we use the pseudo Gray 8PAM constellation. More specifically, if $\hat{\rho}_y$ is smaller than $(r_3 + r_4)/2$, the zeroth bit of \mathbf{b}^{A*} must be 0. The constellation subset associated with the zeroth bit being 1 is $\mathcal{A}_0^{(1)} = \{r_4, r_5, r_6, r_7\}$, and obviously, the point closest to $\hat{\rho}_y$ in $\mathcal{A}_0^{(1)}$ is $r_{0,1}^* = r_4$, which is the same result as that given by Lemma 2. If $\hat{\rho}_y$ is larger than $(r_3 + r_4)/2$, we have $b_0^{A*} = 1$ and $r_{0,0}^* = r_3$, which is also identical to the result given by Lemma 2. Therefore, no error occurs when demapping the zeroth bit using Lemma 2. Demapping the first bit using Lemma 2 has one error interval $((r_3 + r_4)/2, (r_1 + r_6)/2)$, whereas demapping the second bit using Lemma 2 has three error intervals $((r_0 + r_3)/2, (r_1 + r_2)/2)$, $((r_3 + r_4)/2, (r_2 + r_5)/2)$, and $((r_5 + r_6)/2, (r_4 + r_7)/2)$. The LLRs of the first and second bits related to the pseudo 8PAM calculated by the Log-MAP, Max-Log-MAP, and our proposed demapper are shown in Fig. 6. The LLR calculated by our proposed demapper is exactly the same as the Max-Log-MAP demapper when $\hat{\rho}_y$ is outside the error intervals. When $\hat{\rho}_y$ falls within one of the error intervals, the absolute value of the LLR calculated by our proposed demapper is slightly larger than that of the Max-Log-MAP demapper.

3) Error distribution: Since $\phi(x^*, y)$ represents the minimum phase distance between received signal y and the constellation points, we have $\phi(x^*, y) \leq \pi/2^{m_1}$. As the constellation order increases, $\phi(x^*, y)$ tends to 0, and $\cos(\phi(x^*, y))$ tends to 1. For example, in the case of (64 = 16 × 4)-APSK, we have $m_1 = 4$, $\phi(x^*, y) \leq \pi/16 = 0.1963$, and $\cos(\phi(x^*, y)) \geq 0.9808$, whereas in the case of (256 = 32 × 8)-APSK, we have $m_1 = 5$, $\phi(x^*, y) \leq \pi/32 = 0.0982$, and $\cos(\phi(x^*, y)) \geq$

0.9952. Then, $\hat{\rho}_y$ can be approximated by ρ_y , which obeys a Rician distribution. Specifically

$$p(\hat{\rho}_y|r) \approx \frac{2\hat{\rho}_y}{N_0} \exp\left(-\frac{\hat{\rho}_y^2 + r^2}{N_0}\right) I_0\left(\frac{2r\hat{\rho}_y}{N_0}\right) \quad (19)$$

where r denotes the amplitude of transmitted signal x , and $I_0(\cdot)$ is the modified Bessel function of the first kind with order zero.

The error intervals for the 2^{m_2} -ary pseudo PAM can be determined in the following recursive way.

- i) For the zeroth bit and $m_2 \geq 1$, there is no error interval.
- ii) For the first bit and $m_2 = 2$, the error interval is $((r_1 + r_2)/2, (r_0 + r_3)/2)$.
- iii) For the k th bit, where $1 \leq k < m_2$ and $m_2 \geq 2$, there are $2^k - 1$ error intervals. We denote the i th error interval as $(d_{i,1}^{m_2,k}, d_{i,2}^{m_2,k})$, where

$$d_{i,1}^{m_2,k} = \min\left\{\left(r_{e_{i,1}^{m_2,k}} + r_{e_{i,2}^{m_2,k}}\right)/2, \left(r_{e_{i,3}^{m_2,k}} + r_{e_{i,4}^{m_2,k}}\right)/2\right\} \quad (20)$$

$$d_{i,2}^{m_2,k} = \max\left\{\left(r_{e_{i,1}^{m_2,k}} + r_{e_{i,2}^{m_2,k}}\right)/2, \left(r_{e_{i,3}^{m_2,k}} + r_{e_{i,4}^{m_2,k}}\right)/2\right\} \quad (21)$$

and $e_{i,j}^{m_2,k}$ denotes the index of the corresponding radius calculated by (12). For example, for case ii), we have $e_{1,1}^{2,1} = 1$, $e_{1,2}^{2,1} = 2$, $e_{1,3}^{2,1} = 0$, and $e_{1,4}^{2,1} = 3$. In general, index $e_{i,j}^{m_2,k}$ can be recursively determined from $e_{i,j}^{m_2-1,k-1}$ according to

$$e_{i,j}^{m_2,k} = \begin{cases} e_{i,j}^{m_2-1,k-1}, & 1 \leq i \leq 2^{k-1} - 1 \\ 2^{m_2} - 1 - e_{i,j}^{m_2-1,k-1}, & 1 \leq j \leq 4 \\ & 2^{k-1} \leq i < 2^k - 1 \\ 2^{m_2-1} - 1, & 1 \leq j \leq 4 \\ & i = 2^k - 1; j = 1 \\ 2^{m_2-1}, & i = 2^k - 1; j = 2 \\ 2^{m_2-1} - 2^{m_2-k-1} - 1, & i = 2^k - 1; j = 3 \\ 2^{m_2-1} + 2^{m_2-k-1}, & i = 2^k - 1; j = 4. \end{cases} \quad (22)$$

For the product-APSK constellation set \mathcal{X} , each ring has the same number of points, and radius r is uniformly distributed over set \mathcal{A} . Therefore, the probability of $\hat{\rho}_y$ falling into the error interval $(d_{i,1}^{m_2,k}, d_{i,2}^{m_2,k})$ is readily shown to be

$$\begin{aligned} P\left(d_{i,1}^{m_2,k} < \hat{\rho}_y < d_{i,2}^{m_2,k}\right) &= \sum_{s=0}^{2^{m_2}-1} P(r_s) P\left(d_{i,1}^{m_2,k} < \hat{\rho}_y < d_{i,2}^{m_2,k} | r_s\right) \\ &= \frac{1}{2^{m_2}} \sum_{s=0}^{2^{m_2}-1} \int_{d_{i,1}^{m_2,k}}^{d_{i,2}^{m_2,k}} p(\hat{\rho}_y | r_s) d\hat{\rho}_y. \end{aligned} \quad (23)$$

It is clear that (23) does not have a closed-form expression. Fortunately, since the Rician distribution can be approximated by the Gaussian distribution at a high SNR, we have

$$\begin{aligned} P\left(d_{i,1}^{m_2,k} < \hat{\rho}_y < d_{i,2}^{m_2,k}\right) &\approx \frac{1}{2^{m_2}} \sum_{s=0}^{2^{m_2}-1} \left(Q\left(\frac{d_{i,1}^{m_2,k} - r_s}{\sqrt{N_0/2}}\right) - Q\left(\frac{d_{i,2}^{m_2,k} - r_s}{\sqrt{N_0/2}}\right) \right) \end{aligned} \quad (24)$$

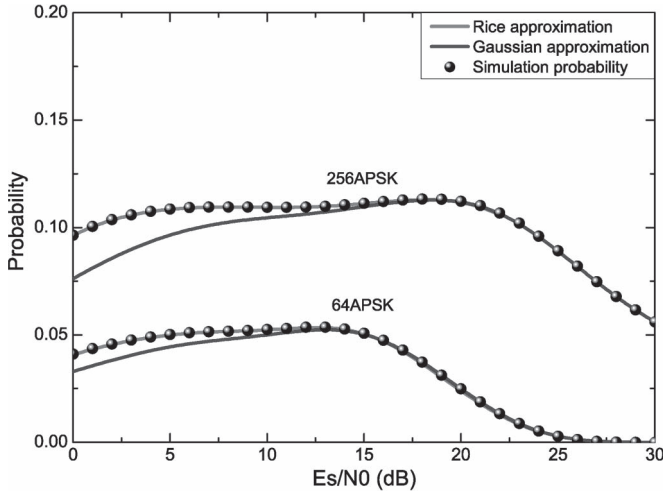


Fig. 7. Probability of $\hat{\rho}_y$ falling into the error interval(s) for $(64 = 16 \times 4)$ -APSK and $(256 = 32 \times 8)$ -APSK, for the AWGN channel.

and the probability of $\hat{\rho}_y$ falling into the error intervals can be obtained by

$$P_e \approx \frac{1}{2^{m_2}} \times \sum_{s=0}^{2^{m_2}-1} \sum_{k=1}^{m_2-1} \sum_{i=1}^{2^k-1} \left(Q\left(\frac{d_{i,1}^{m_2,k} - r_s}{\sqrt{N_0/2}}\right) - Q\left(\frac{d_{i,2}^{m_2,k} - r_s}{\sqrt{N_0/2}}\right) \right) \quad (25)$$

where $Q(x) = (1/\sqrt{2\pi}) \int_x^\infty \exp(-u^2/2) du$ represents the standard tail probability function of the Gaussian distribution with zero mean and unity variance.

For the case of $(64 = 16 \times 4)$ -APSK, the probability of $\hat{\rho}_y$ falling into the error interval is shown in Fig. 7, as the function of the SNR $= E_s/N_0$ over the AWGN channel. Three P_e 's are shown in Fig. 7, namely, the two theoretical P_e 's derived by the Rician and Gaussian approximations and the probability P_e obtained by simulation. It can be observed that the probability of $\hat{\rho}_y$ falling into the error interval is quite small even at low SNRs. At high SNRs, the Gaussian approximation matches well with the simulation result, and probability P_e tends to zero with the increase in the SNR. This is due to the fact that received signal y is likely to be very close to transmitted signal x at a high SNR, and consequently, the probability of $\hat{\rho}_y$ falling into the error interval becomes extremely small.

Fig. 7 also shows the probability of $\hat{\rho}_y$ falling into the error intervals for $(256 = 32 \times 8)$ -APSK for transmission over the AWGN channel at different SNR values. Probability P_e is much higher than that of 64-APSK, since 256-APSK has more error intervals, but it is no more than 12% at low SNRs. At high SNRs, the Gaussian approximation matches well with the simulation result, and the probability decreases with the increase in the SNR. Probability P_e tends to zero, given a sufficiently high SNR value, which is outside the SNR region shown in Fig. 7.

Our theoretical analysis of $(64 = 16 \times 4)$ -APSK and $(256 = 32 \times 8)$ -APSK, therefore, shows that the error caused by the proposed simplified demapper is relatively small compared

with the accurate LLR, and the probability of $\hat{\rho}_y$ falling into the error intervals is also small (less than 6% for 64-APSK and less than 12% for 256-APSK). Moreover, probability P_e tends to zero at a sufficiently high SNR value. We can conclude that the performance degradation associated with the proposed demapper is negligible for $(64 = 16 \times 4)$ -APSK and $(256 = 32 \times 8)$ -APSK, in comparison with that of the Max-Log-MAP demapper. This will be further demonstrated by the bit error rate (BER) simulation results in Section IV.

It should be noted that Lemma 2 and 3 can be implemented with the aid of a lookup table that defines the interval of y and identifies which particular k_i^* is used for each of the intervals specified by a set of thresholds. For nonuniform constellations such as product-APSK, we can use a larger lookup table, which contains the additional error intervals required for maintaining the performance, albeit this requires more comparison operations and an increased storage capacity.

IV. SIMULATION RESULTS

The BER performance of the proposed soft demapper was evaluated by simulation. According to our analysis presented in the previous sections, the proposed soft demapper achieves exactly the same performance as the standard Max-Log-MAP demapper for Gray-labeled PAM, PSK, and QAM. By contrast, it suffers from a slight performance loss for the Gray-labeled product-APSK because of the nonuniformly spaced pseudo PAM constellation embedded in the product-APSK. We therefore carried out simulations for the QAM and product-APSK constellations. The simulation parameters are listed as follows.

- Constellation Labeling: gray-labeled 64QAM, $(64 = 16 \times 4)$ -APSK, 256QAM and $(256 = 32 \times 8)$ -APSK;
- Demapper: the standard Max-Log-MAP demapper and the proposed simplified soft demapper;
- Decoder: the 1/2-rate 64 800-bit long low-density parity-check (LDPC) code of DVB-T2 was employed, whereby the normalized Min-Sum decoding algorithm with a normalization factor of $\alpha = 1/0.875$ was selected [22]. The maximum number of LDPC iterations was set to 50;
- Channel: AWGN and independent identically distributed Rayleigh fading channels.

The achievable BER performance is shown in Figs. 8 and 9 for the AWGN and Rayleigh fading channels, respectively. It can be observed that the BER curves obtained by the Max-Log-MAP and our simplified demappers are overlapped for the Gray-labeled 64QAM and 256QAM over both the AWGN and Rayleigh fading channels. This confirms that the soft information calculated by our proposed demapper is exactly the same as that of the Max-Log-MAP demapper. The results shown in Figs. 8 and 9 also confirm that for the Gray-labeled product-APSK, the performance degradation caused by the proposed demapper is negligible compared with the Max-Log-MAP demapper. Specifically, at the BER of 10^{-5} , the performance loss is below 0.05 dB for the Gray-labeled 64APSK and 256APSK over both AWGN and Rayleigh channels, as shown in Figs. 8 and 9. As expected, the performance degradation in the case of $(256 = 32 \times 8)$ -APSK is slightly higher than that of the $(64 = 16 \times 4)$ -APSK, owing to the fact that 256APSK

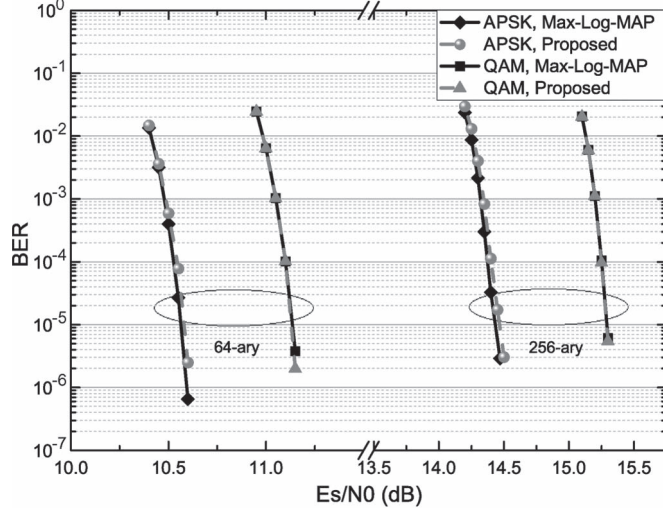


Fig. 8. BER performance comparison over the AWGN channel.

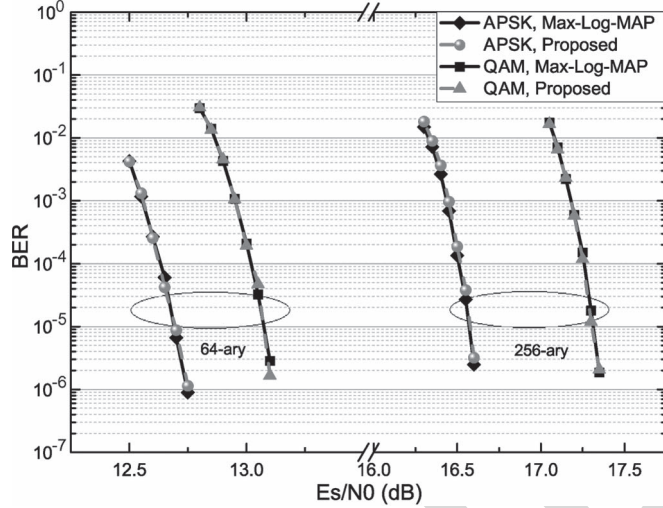


Fig. 9. BER performance comparison over the Rayleigh fading channel.

627 has one more bit related to the pseudo PAM. However, the
628 performance loss still remains below 0.05 dB for 256APSK.

629

V. CONCLUSION

630 In this paper, a universal simplified soft demapper has been
631 proposed for various binary-reflected Gray-labeled constella-
632 tions. For the constellation of size 2^m , our proposed demap-
633 per imposes a low-complexity order of $O(m)$, instead of the
634 complexity order of $O(2^m)$ imposed by the standard Max-Log-
635 MAP demapper. Our theoretical analysis and simulation results
636 have shown that the proposed simplified demapper achieves
637 exactly the same performance as that of the Max-Log-MAP
638 solution for Gray-labeled PAM, PSK, and QAM, whereas for
639 the Gray-labeled product-APSK, the performance degradation
640 caused by our simplified demapper remains negligible com-
641 pared with that of the Max-Log-MAP demapper. More particu-
642 larly, we have verified that this performance loss is less than
643 0.05 dB for both (64 = 16 × 4)-APSK and (256 = 32 × 8)-
644 APSK for transmission over both the AWGN and Rayleigh
645 fading channels.

APPENDIX A

PROOF OF LEMMA 2

646 Once x^* and \mathbf{b}^* are determined, constellation subset $\mathcal{X}_i^{(\bar{b}_i^*)}$ 648
649 can be written as

$$\mathcal{X}_i^{(\bar{b}_i^*)} = \{x_k | x_k \in \mathcal{X}, c_{i-1}^k \oplus c_i^k = \bar{b}_i^*\} \quad (26)$$

where $\mathbf{c}^k = (c_0^k c_1^k \dots c_{m-1}^k)$ denotes the binary representation 650
of k , and we have $c_{-1}^k = 0$. By denoting the nearest constella- 651
tion point to x^* in subset $\mathcal{X}_i^{(\bar{b}_i^*)}$ as the k_i^* th constellation point 652
 $x_{k_i^*}$, we have 653

$$x_{k_i^*} = \arg \min_{x \in \mathcal{X}_i^{(\bar{b}_i^*)}} |x^* - x| \quad (27)$$

$$k_i^* = \arg \min_{k \in \mathcal{K}_i^{(\bar{b}_i^*)}} |k^* - k| \quad (28)$$

where $\mathcal{K}_i^{(\bar{b}_i^*)} = \{k | 0 \leq k < 2^m, c_{i-1}^k \oplus c_i^k = \bar{b}_i^*\}$ denotes the 654
index set corresponding to $\mathcal{X}_i^{(\bar{b}_i^*)}$. 655

For $k \in \mathcal{K}_i^{(\bar{b}_i^*)}$, we can express k as $k = \sum_{j=0}^{m-1} c_j^k 2^{m-j-1}$, 656
where we have $c_{i-1}^k \oplus c_i^k = \bar{b}_i^* = \bar{c}_{i-1}^{k^*} \oplus c_i^{k^*}$. Therefore, 657
we have 658

$$c_{i-1}^k = \bar{c}_{i-1}^{k^*} \text{ and } c_i^k = c_i^{k^*} \text{ or } c_{i-1}^k = c_{i-1}^{k^*} \text{ and } c_i^k = \bar{c}_i^{k^*}. \quad (29)$$

We now discuss the two situations. 659

i) The case of $c_{i-1}^k = \bar{c}_{i-1}^{k^*}$ and $c_i^k = c_i^{k^*}$. We have $c_{i-1}^{k^*} - 660$
 $c_{i-1}^k = \pm 1$, and 661

$$\begin{aligned} & \left| \sum_{j_1=0}^{i-2} (c_{j_1}^{k^*} - c_{j_1}^k) 2^{m-j_1-1} + (c_{i-1}^{k^*} - c_{i-1}^k) 2^{m-i} \right| \\ &= 2^{m-i} \left| \sum_{j_1=0}^{i-2} (c_{j_1}^{k^*} - c_{j_1}^k) 2^{i-j_1-1} + (c_{i-1}^{k^*} - c_{i-1}^k) \right| \\ &\geq 2^{m-i} \end{aligned} \quad (30)$$

where the inequality follows from the fact that 662
 $\sum_{j_1=0}^{i-2} (c_{j_1}^{k^*} - c_{j_1}^k) 2^{i-j_1-1}$ must be even and that 663
 $c_{i-1}^{k^*} - c_{i-1}^k$ is odd. We also have 664

$$\begin{aligned} & \left| \sum_{j_2=i+1}^{m-1} (c_{j_2}^{k^*} - c_{j_2}^k) 2^{m-j_2-1} \right| \leq \sum_{j_2=i+1}^{m-1} |c_{j_2}^{k^*} - c_{j_2}^k| 2^{m-j_2-1} \\ &\leq \sum_{j_2=i+1}^{m-1} 2^{m-j_2-1} = 2^{m-i-1} - 1. \end{aligned} \quad (31)$$

Then, we can find the lower bound of $|k^* - k|$ as 665

$$\begin{aligned} |k^* - k| &= \left| \sum_{j_1=0}^{i-2} (c_{j_1}^{k^*} - c_{j_1}^k) 2^{m-j_1-1} + (c_{i-1}^{k^*} - c_{i-1}^k) 2^{m-i} \right. \\ &\quad \left. + \sum_{j_2=i+1}^{m-1} (c_{j_2}^{k^*} - c_{j_2}^k) 2^{m-j_2-1} \right| \\ &\geq |2^{m-i} - (2^{m-i-1} - 1)| = 2^{m-i-1} + 1. \end{aligned} \quad (32)$$

666 ii) The case of $c_{i-1}^k = c_{i-1}^{k^*}$ and $c_i^k = \overline{c_i^{k^*}}$. If $\exists j_1 \in$
 667 $\{0, 1, \dots, i-2\}$, which makes $c_{j_1}^k \neq c_{j_1}^{k^*}$, then we have

$$\begin{aligned} |k^* - k| &= \left| \sum_{j_1=0}^{i-2} (c_{j_1}^{k^*} - c_{j_1}^k) 2^{m-j_1-1} \right. \\ &\quad \left. + \sum_{j_2=i}^{m-1} (c_{j_2}^{k^*} - c_{j_2}^k) 2^{m-j_2-1} \right| \\ &\geq \left| \sum_{j_1=0}^{i-2} (c_{j_1}^{k^*} - c_{j_1}^k) 2^{m-j_1-1} \right| \\ &\quad - \left| \sum_{j_2=i}^{m-1} (c_{j_2}^{k^*} - c_{j_2}^k) 2^{m-j_2-1} \right| \\ &\geq |2^{m-i+1} - (2^{m-i} - 1)| = 2^{m-i} + 1. \end{aligned} \quad (33)$$

668 On the other hand, if $c_{j_1}^k = c_{j_1}^{k^*}$ for $0 \leq j_1 \leq i-2$,
 669 we have

$$\begin{aligned} |k^* - k| &= \left| \left(c_i^{k^*} - \overline{c_i^{k^*}} \right) 2^{m-i-1} + \sum_{j_2=i+1}^{m-1} (c_{j_2}^{k^*} - c_{j_2}^k) 2^{m-j_2-1} \right| \\ &= 2^{m-i-1} - (-1)^{c_i^{k^*}} \sum_{j_2=i+1}^{m-1} c_{j_2}^{k^*} 2^{m-j_2-1} \\ &\quad + (-1)^{c_i^{k^*}} \sum_{j_2=i+1}^{m-1} c_{j_2}^k 2^{m-j_2-1}. \end{aligned} \quad (34)$$

670 Apparently, the minimum of (34) is smaller than 2^{m-i-1} and,
 671 thus, smaller than both the lower bounds given in (32) and (33).
 672 Since the first two items in (34) are fixed, minimizing $|k^* -$
 673 $k|$ is equivalent to minimizing $(-1)^{c_i^{k^*}} \sum_{j_2=i+1}^{m-1} c_{j_2}^{k^*} 2^{m-j_2-1}$.
 674 Therefore, we have $c_j^{k^*} = c_i^{k^*}$, $i+1 \leq j \leq m-1$, and

$$\begin{aligned} k_i^* &= \sum_{j_1=0}^{i-2} c_{j_1}^{k^*} 2^{m-j_1-1} + \overline{c_i^{k^*}} 2^{m-i-1} + \sum_{j_2=i+1}^{m-1} c_{j_2}^{k^*} 2^{m-j_2-1} \\ &= 2^{m-i-1} - c_i^{k^*} + \sum_{j=0}^{i-1} c_j^{k^*} 2^{m-j-1}. \end{aligned} \quad (35)$$

675 It is clear that k_i^* is the unique solution of (28). Hence, $\forall k \in$
 676 $\mathcal{K}_i^{(\overline{b_i^*})} \setminus \{k_i^*\}$, we have $|k^* - k| \geq |k^* - k_i^*| + 1$, and

$$|x^* - x_k| \geq |x^* - x_{k_i^*}| + \delta. \quad (36)$$

677 Since x^* is the nearest constellation point to y , we obtain

$$|y - hx^*| \leq |h|\delta/2 \quad (37)$$

for $y \in [-2^{m-1}|h|\delta, 2^{m-1}|h|\delta]$. In this case, for $k \in \mathcal{K}_i^{(\overline{b_i^*})} \setminus$
 678 $\{k_i^*\}$, we have 679

$$\begin{aligned} |y - hx_k| &\geq |h(x^* - x_k)| - |y - hx^*| \\ &\geq |h|(|x^* - x_{k_i^*}| + \delta) - |h|\delta/2 \\ &\geq |h(x^* - x_{k_i^*})| + |y - hx^*| \geq |y - hx_{k_i^*}|. \end{aligned} \quad (38)$$

It is easy to find that this inequality still holds when y is outside
 680 the interval $[-2^{m-1}|h|\delta, 2^{m-1}|h|\delta]$. Therefore, $x_{k_i^*}$ is not only
 681 the nearest constellation point to x^* in $\mathcal{X}_i^{(\overline{b_i^*})}$ but the nearest
 682 constellation point to y in $\mathcal{X}_i^{(\overline{b_i^*})}$ as well. This completes the
 683 proof of Lemma 2. ■ 684

APPENDIX B

PROOF OF THE TRIANGLE INEQUALITY OF THE PHASE DISTANCE

From (8), $\phi(x, y)$ can be rewritten as $\phi(x, y) = \min\{|\varphi_x -$
 688 $\varphi_y|, 2\pi - |\varphi_x - \varphi_y|\}$. The proof is divided into three parts
 689 according to the values of $|\varphi_x - \varphi_y|$ and $|\varphi_y - \varphi_z|$. 690

i) If $|\varphi_x - \varphi_y| \leq \pi$ and $|\varphi_y - \varphi_z| \leq \pi$, we have 691

$$\phi(x, y) + \phi(y, z) = |\varphi_x - \varphi_y| + |\varphi_y - \varphi_z| \geq |\varphi_x - \varphi_z| \geq \phi(x, z). \quad (39)$$

ii) For $|\varphi_x - \varphi_y| > \pi$ and $|\varphi_y - \varphi_z| \leq \pi$ or $|\varphi_x - \varphi_y| \leq \pi$
 692 and $|\varphi_y - \varphi_z| > \pi$, without loss of generality, we assume
 693 $|\varphi_x - \varphi_y| > \pi$ and $|\varphi_y - \varphi_z| \leq \pi$. Then, we have 694

$$\begin{aligned} \phi(x, y) + \phi(y, z) &= 2\pi - |\varphi_x - \varphi_y| + |\varphi_y - \varphi_z| \\ &\geq 2\pi - |\varphi_x - \varphi_z| \geq \phi(x, z). \end{aligned} \quad (40)$$

iii) For $|\varphi_x - \varphi_y| > \pi$ and $|\varphi_y - \varphi_z| > \pi$, without loss of
 695 generality, we assume $\varphi_x \geq \varphi_z$. Since φ_x, φ_y , and φ_z are
 696 all inside the interval $[0, 2\pi]$, we have $\varphi_x \geq \varphi_z > \varphi_y + \pi$
 697 or $\varphi_z \leq \varphi_x < \varphi_y - \pi$. If $\varphi_x \geq \varphi_z > \varphi_y + \pi$, we have 698

$$|\varphi_x - \varphi_y| + |\varphi_y - \varphi_z| + |\varphi_x - \varphi_z| = 2\varphi_x - 2\varphi_y < 4\pi. \quad (41)$$

If $\varphi_z \leq \varphi_x < \varphi_y - \pi$, we have 699

$$|\varphi_x - \varphi_y| + |\varphi_y - \varphi_z| + |\varphi_x - \varphi_z| = 2\varphi_y - 2\varphi_z < 4\pi. \quad (42)$$

In both cases, we have 700

$$\begin{aligned} \phi(x, y) + \phi(y, z) &= 2\pi - |\varphi_x - \varphi_y| + 2\pi - |\varphi_y - \varphi_z| > |\varphi_x - \varphi_z| \\ &\geq \phi(x, z). \end{aligned} \quad (43)$$

This completes the proof. ■ 701

APPENDIX C

PROOF OF LEMMA 3

The definitions of $\mathcal{X}_i^{(\overline{b_i^*})}$ and $x_{k_i^*}$ are the same as given in
 704 (26) and (27). Noting that 705

$$\begin{aligned} |x^* - x|^2 &= \left| \sqrt{E_s} \exp(j\varphi_{x^*}) - \sqrt{E_s} \exp(j\varphi_x) \right|^2 \\ &= 2E_s - 2E_s \cos(\phi(x^*, x)) \end{aligned} \quad (44)$$

706 we have

$$k_i^* = \arg \min_{k \in \mathcal{K}_i^{(\bar{b}_i^*)}} \phi(x_k^*, x_k). \quad (45)$$

707 Similar to the proof of Lemma 2, we can get the unique solution
708 of k_i^* as shown in (11), which means that $\forall k \in \mathcal{K}_i^{(\bar{b}_i^*)} \setminus \{k_i^*\}$,
709 we have

$$\phi(x_k, x^*) \geq \phi(x^*, x_{k_i^*}) + 2\pi/2^m. \quad (46)$$

710 Since x^* is the nearest constellation point to y , we obtain

$$\phi(x^*, y) \leq \pi/2^m. \quad (47)$$

711 According to (7), (9), (46), and (47), we have, $\forall k \in \mathcal{K}_i^{(\bar{b}_i^*)} \setminus \{k_i^*\}$

$$\begin{aligned} \phi(x_k, y) &\geq \phi(x^*, x_k) - \phi(x^*, y) \\ &\geq \phi(x^*, x_{k_i^*}) + 2\pi/2^m - \pi/2^m \\ &\geq \phi(x^*, x_{k_i^*}) + \phi(x^*, y) \geq \phi(x_{k_i^*}, y) \end{aligned} \quad (48)$$

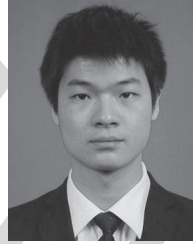
$$|y - hx_k| \geq |y - hx_{k_i^*}|. \quad (49)$$

712 Therefore, $x_{k_i^*}$ is not only the nearest constellation point to x^*
713 in $\mathcal{X}_i^{(\bar{b}_i^*)}$ but the nearest constellation point to y in $\mathcal{X}_i^{(\bar{b}_i^*)}$ as well.
714 This completes the proof. ■

REFERENCES

- 716 [1] *Digital Video Broadcasting (DVB); Frame Structure Channel Coding and*
717 *Modulation for a Second Generation Digital Terrestrial Television Broad-*
718 *casting System (DVB-T2)*, ETSI EN Std. 302 755 V1.3.1, Apr. 2012.
- 719 [2] *Digital Video Broadcasting (DVB); Frame Structure Channel Coding and*
720 *Modulation for a Second Generation Digital Transmission System for*
721 *Cable Systems (DVB-C2)*, ETSI EN Std. 302 769 V1.2.1, Apr. 2012.
- 722 [3] Third-Generation Partnership Project (3GPP); Technical specification
723 group radio access network; Physical layer aspects for evolved UTRA,
724 Third-Generation Partnership Project (3GPP), Sophia Antipolis, France.
725 [Online]. Available: <http://www.3gpp.org/ftp/Specs/html-info/25814.htm>
- 726 [4] J. Erfanian, S. Pasupathy, and G. Gulak, "Reduced complexity symbol de-
727 tectors with parallel structures for ISI channels," *IEEE Trans. Commun.*,
728 vol. 42, no. 2/3/4, pp. 1661–1671, Feb./Mar./Apr. 1994.
- 729 [5] P. Robertson, E. Villebrun, and P. Hoeher, "A comparison of optimal
730 and sub-optimal MAP decoding algorithms operating in the log domain,"
731 in *Proc. IEEE ICC*, Seattle, WA, USA, Jun. 18–22, 1995, vol. 2,
732 pp. 1009–1013.
- 733 [6] L. Wang, D. Xu, and X. Zhang, "Recursive bit metric generation for PSK
734 signals with Gray labeling," *IEEE Commun. Lett.*, vol. 16, no. 2, pp. 180–
735 182, Feb. 2012.
- 736 [7] E. Akay and E. Ayanoglu, "Low complexity decoding of bit-interleaved
737 coded modulation for M-ary QAM," in *Proc. IEEE ICC*, Paris, France,
738 Jun. 20–24, 2004, vol. 2, pp. 901–905.
- 739 [8] C.-W. Chang, P.-N. Chen, and Y. S. Han, "A systematic bit-wise decom-
740 position of M-ary symbol metric," *IEEE Trans. Wireless Commun.*, vol. 5,
741 no. 10, pp. 2742–2751, Oct. 2006.
- 742 [9] F. Tosato and P. Bisaglia, "Simplified soft-output demapper for binary
743 interleaved COFDM with application to HIPERLAN/2," in *Proc. IEEE*
744 *ICC*, New York, NY, USA, Apr. 28/May 2, 2002, vol. 2, pp. 664–668.
- 745 [10] M. Zhang and S. Kim, "Efficient soft demapping for M-ary APSK," in
746 *Proc. ICTC*, Seoul, Korea, Sep. 28–30, 2011, pp. 641–644.
- 747 [11] G. Gül, A. Vargas, W. H. Gerstacker, and M. Breiling, "Low complex-
748 ity demapping algorithms for multilevel codes," *IEEE Trans. Commun.*,
749 vol. 59, no. 4, pp. 998–1008, Apr. 2011.
- 750 [12] J. W. Park, M. H. Sunwoo, P. S. Kim, and D.-I. Chang, "Low complexity
751 soft-decision demapper for high order modulation of DVB-S2 system," in
752 *Proc. ISOCC*, Busan, Korea, Nov. 24, 2008, pp. II-37–II-40.
- 753 [13] D. Pérez-Calderoñ, V. Baena-Lecuyer, A. C. Oria, P. López, and
754 J. G. Doblado, "Rotated constellation demapper for DVB-T2," *Electron.*
755 *Lett.*, vol. 47, no. 1, pp. 31–32, Jan. 2011.
- 756 [14] S. Tomasin and M. Butussi, "Low complexity demapping of rotated and
757 cyclic Q delayed constellations for DVB-T2," *IEEE Wireless Commun.*
758 *Lett.*, vol. 1, no. 2, pp. 81–84, Apr. 2012.

- [15] Y. Fan and C. Tsui, "Low-complexity rotated QAM demapper for the
iterative receiver targeting DVB-T2 standard," in *Proc. IEEE VTC-Fall*,
Québec City, QC, Canada, Sep. 3–6, 2012, pp. 1–5.
- [16] Z. Liu, Q. Xie, K. Peng, and Z. Yang, "APSK constellation with
Gray mapping," *IEEE Commun. Lett.*, vol. 15, no. 12, pp. 1271–1273,
Dec. 2011.
- [17] Q. Xie, Z. Wang, and Z. Yang, "Simplified soft demapper for APSK with
product constellation labeling," *IEEE Trans. Wireless Commun.*, vol. 11,
no. 7, pp. 2649–2657, Jul. 2012.
- [18] F. Gray, "Pulse code communications," US Patent 2632058, Mar. 17,
1953.
- [19] E. Agrell, J. Lassing, E. G. Ström, and T. Ottosson, "On the optimality of
the binary reflected Gray code," *IEEE Trans. Inf. Theory*, vol. 50, no. 12,
pp. 3170–3182, Dec. 2004.
- [20] E. M. Reingold, J. Nievergelt, and N. Deo, *Combinatorial Algorithms: The-
ory and Practice*. Englewood Cliffs, NJ, USA: Prentice-Hall, 1977.
- [21] R. De Gaudenzi, A. Guillen, and A. Martinez, "Performance analysis of
turbo-coded APSK modulations over nonlinear satellite channels," *IEEE*
Trans. Wireless Commun., vol. 5, no. 9, pp. 2396–2407, Sep. 2006.
- [22] J. Chen and M. P. C. Fossorier, "Near optimum universal belief propa-
gation based decoding of low-density parity check codes," *IEEE Trans.*
Commun., vol. 50, no. 3, pp. 406–414, Mar. 2002.



Qi Wang received the B.S. degree from Tsinghua University, Beijing, China, in 2011, where he is currently working toward the Ph.D. degree with the Department of Electronic Engineering. His current research interests include optical wireless communications and channel coding and modulation.



Qiuliang Xie received the B.Eng. degree in telecommunication engineering from Beijing University of Posts and Telecommunications, Beijing, China, in 2006 and the Ph.D. degree in electronic engineering from Tsinghua University, Beijing, in 2011, both with high honors.

From July 2011 to March 2013, he was with Digital TV National Engineering Laboratory (Beijing) Co., Ltd., where he participated in developing China's next-generation broadcasting standard. He is currently a Postdoctoral Fellow with the Department

of Radiation Oncology, University of California, Los Angeles, CA, USA, where he is engaged in medical image processing. His main research interests include medical image processing and broadband wireless communication, specially including information theory, coding theory, and image/signal processing theories.

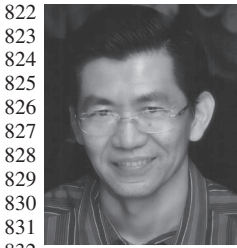


Zhaocheng Wang (SM'10) received the B.S., M.S., and Ph.D. degrees from Tsinghua University, Beijing, China, in 1991, 1993, and 1996, respectively.

From 1996 to 1997, he was a Postdoctoral Fellow with Nanyang Technological University, Singapore. From 1997 to 1999, he was with OKI Techno Centre (Singapore) Pte. Ltd., first as a Research Engineer and then as a Senior Engineer. From 1999 to 2009, he was with Sony Deutschland GmbH, first as a Senior Engineer and then as a Principal Engineer. He is

currently a Professor with the Department of Electronic Engineering, Tsinghua University. He has published over 80 technical papers. He is the holder of 30 U.S./European Union patents. His research interests include wireless communications, digital broadcasting, and millimeter-wave communications.

Dr. Wang has served as a Technical Program Committee Cochair/Member of many international conferences. He is a Fellow of the Institution of Engineering and Technology.



Sheng Chen (M'90–SM'97–F'08) received the B.Eng. degree in control engineering from East China Petroleum Institute, Dongying, China, in 1982; the Ph.D. degree in control engineering from City University London, London, U.K., in 1986; and the D.Sc. degree from the University of Southampton, Southampton, U.K., in 2005.

From 1986 to 1999, he held research and academic appointments with The University of Sheffield, The University of Edinburgh, and the University of Portsmouth, all in the U.K. Since 1999, he has been

with Electronics and Computer Science, University of Southampton, where he is currently a Professor of intelligent systems and signal processing. He is a Distinguished Adjunct Professor with King Abdulaziz University, Jeddah, Saudi Arabia. He has published over 480 research papers. His recent research interests include adaptive signal processing, wireless communications, modeling and identification of nonlinear systems, neural network and machine learning, intelligent control system design, evolutionary computation methods, and optimization.

Dr. Chen is a Chartered Engineer and a Fellow of the Institution of Engineering and Technology. He was an Institute for Scientific Information highly cited researcher in the engineering category in March 2004.



Lajos Hanzo Lajos Hanzo (M'91–SM'92–F'04) received the M.S. degree (with first-class honors) in electronics and the Ph.D. degree from the Technical University of Budapest, Budapest, Hungary, in 1976 and 1983, respectively, the D.Sc. degree from the University of Southampton, Southampton, U.K., in 2004, and the "Doctor Honoris Causa" degree from the Technical University of Budapest in 2009.

During his 35-year career in telecommunications, he has held various research and academic posts in Hungary, Germany, and the U.K. Since 1986, he has

been with the School of Electronics and Computer Science, University of Southampton, Southampton, U.K., where he holds the Chair for Telecommunications. Since 2009, he has been a Chaired Professor with Tsinghua University, Beijing China. He is currently directing a 100-strong academic research team, working on a range of research projects in the field of wireless multimedia communications sponsored by industry; the Engineering and Physical Sciences Research Council, U.K.; the European IST Programme; and the Mobile Virtual Centre of Excellence, U.K. He is an enthusiastic supporter of industrial and academic liaison and offers a range of industrial courses. He has successfully supervised 80 Ph.D. students, coauthored 20 John Wiley/IEEE Press books on mobile radio communications totaling in excess of 10 000 pages, published more than 1250 research entries on IEEE Xplore, and presented keynote lectures. (For further information on research in progress and associated publications, please refer to <http://www-mobile.ecs.soton.ac.uk>.)

Dr. Hanzo is Fellow of the Royal Academy of Engineering, U.K., a Fellow of the Institution of Electrical Engineers, and a Governor of the IEEE Vehicular Technology Society. He has been a Technical Program Committee Chair and a General Chair for IEEE conferences. During 2008–2012, he was the Editor-in-Chief of the IEEE Press. He has received a number of distinctions.

AUTHOR QUERIES

AUTHOR PLEASE ANSWER ALL QUERIES

AQ1 = Note that “in the performance analysis section” was changed to “in Section III-D.4.”

AQ2 = Note that the section heading “The case of $(64 = 16 \times 4)$ -APSK” was changed to “ $(64 = 16 \times 4)$ -APSK” here and in another similar instance.

END OF ALL QUERIES

IEEE
Proof